

The protonmotive force and respiratory control:

Building blocks of mitochondrial physiology

Part 1.

http://www.mitoeagle.org/index.php/MitoEAGLE_preprint_2017-09-21

Preprint version 12 (2017-10-21)

MitoEAGLE Network

Corresponding author: Gnaiger E

Contributing co-authors

Ahn B, Alves MG, Amati F, Åsander Frostner E, Bailey DM, Bastos Sant'Anna Silva AC, Battino M, Beard DA, Ben-Shachar D, Bishop D, Breton S, Brown GC, Brown RA, Buettner GR, Carvalho E, Cervinkova Z, Chang SC, Chicco AJ, Coen PM, Collins JL, Crisóstomo L, Davis MS, Dias T, Distefano G, Doerrier C, Ehinger J, Elmer E, Fell DA, Ferko M, Ferreira JCB, Filipovska A, Fisher J, Garcia-Roves PM, Garcia-Souza LF, Genova ML, Gonzalo H, Goodpaster BH, Gorr TA, Han J, Harrison DK, Hellgren KT, Hernansanz P, Holland O, Hoppel CL, Iglesias-Gonzalez J, Irving BA, Iyer S, Jackson CB, Jansen-Dürr P, Jespersen NR, Jha RK, Kaambre T, Kane DA, Kappler L, Keijer J, Komlodi T, Kopitar-Jerala N, Krakovcic N, Kuang J, Labieniec-Watala M, Lai N, Laner V, Lee HK, Lemieux H, Lerfall J, Lucchinetti E, MacMillan-Crow LA, Makrecka-Kuka M, Meszaros AT, Moiso N, Molina AJA, Montaigne D, Moore AL, Murray AJ, Newsom S, Nozickova K, O'Gorman D, Oliveira PF, Oliveira PJ, Orynbayeva Z, Pak YK, Palmeira CM, Patel HH, Pesta D, Petit PX, Pichaud N, Pirkmajer S, Porter RK, Pranger F, Prochownik EV, Radenkovic F, Reboredo P, Renner Sattler K, Robinson MM, Rohlena J, Røslund GV, Rossiter HB, Salvadego D, Scatena R, Schartner M, Scheibye-Knudsen M, Schilling JM, Schlattner U, Schoenfeld P, Scott GR, Singer D, Sobotka O, Spinazzi M, Stier A, Stocker R, Sumbalova Z, Suravajhala P, Tanaka

27 M, Tandler B, Tepp K, Tomar D, Towheed A, Trivigno C, Tronstad KJ, Trougakos IP,
28 Tyrrell DJ, Velika B, Vendelin M, Vercesi AE, Victor VM, Ward ML, Watala C, Wei YH,
29 Wieckowski MR, Wohlwend M, Wolff J, Wuest RCI, Zaugg K, Zaugg M, Zorzano A

30

31 Supporting co-authors:

32 Arandarčikaitė O, Bakker BM, Bernardi P, Boetker HE, Borsheim E, Borutaitė V, Bouitbir J,
33 Calabria E, Calbet JA, Chaurasia B, Clementi E, Coker RH, Collin A, Das AM, De Palma C,
34 Dubouchaud H, Duchon MR, Durham WJ, Dyrstad SE, Engin AB, Fornaro M, Gan Z, Garlid
35 KD, Garten A, Gourlay CW, Granata C, Haas CB, Haavik J, Haendeler J, Hand SC, Hepple
36 RT, Hickey AJ, Hoel F, Kainulainen H, Keppner G, Khamoui AV, Klingenspor M, Koopman
37 WJH, Kowaltowski AJ, Krajcova A, Lenaz G, Malik A, Markova M, Mazat JP, Menze MA,
38 Methner A, Muntané J, Muntean DM, Neuzil J, Oliveira MT, Pallotta ML, Parajuli N,
39 Pettersen IKN, Pulinilkunnil T, Ropelle ER, Salin K, Sandi C, Sazanov LA, Siewiera K,
40 Silber AM, Skolik R, Smenes BT, Soares FAA, Sokolova I, Sonkar VK, Stankova P,
41 Swerdlow RH, Szabo I, Trifunovic A, Thyfault JP, Tretter L, Vieyra A, Votion DM, Williams

42

C

43

44

Updates:

45

http://www.mitoeagle.org/index.php/MitoEAGLE_preprint_2017-09-21

46

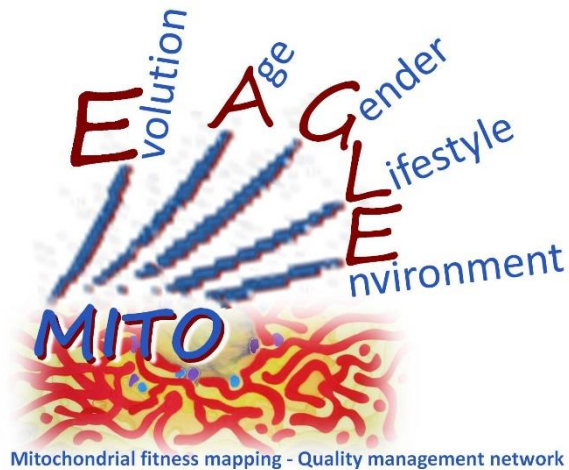
Correspondence: Gnaiger E

Department of Visceral, Transplant and Thoracic Surgery, D. Swarovski Research Laboratory, Medical University of Innsbruck, Innrain 66/4, A-6020 Innsbruck, Austria

Email: erich.gnaiger@i-med.ac.at

Tel: +43 512 566796, Fax: +43 512 566796 20

This manuscript on 'The protonmotive force and respiratory control' is a position statement in the frame of COST Action CA15203 MitoEAGLE. The list of co-authors evolved from MitoEAGLE Working Group Meetings and a **bottom-up** spirit of COST in phase 1: This is an open invitation to scientists and students to join as co-authors, to provide a balanced view on mitochondrial respiratory control, a fundamental introductory presentation of the concept of the protonmotive force, and a consensus statement on reporting data of mitochondrial respiration in terms of metabolic flows and fluxes. We plan a series of follow-up reports by the expanding MitoEAGLE Network, to increase the scope of recommendations on harmonization and facilitate global communication and collaboration.



Phase 2: MitoEAGLE preprint (Versions 01 – 10): We continue to invite comments and suggestions on the, particularly if you are an **early career investigator adding an open future-oriented perspective**, or an **established scientist providing a balanced historical basis**. Your critical input into the quality of the manuscript will be most welcome, improving our aims to be educational, general, consensus-oriented, and practically helpful for students working in mitochondrial respiratory physiology.

Phase 3 (2017-11-11): Manuscript submission to a preprint server, such as BioRxiv. We want to invite further opinion leaders: To join as a co-author, please feel free to focus on a particular section in terms of direct input and references, contributing to the scope of the manuscript from the perspective of your expertise. Your comments will be largely posted on the discussion page of the MitoEAGLE preprint website.

If you prefer to submit comments in the format of a referee's evaluation rather than a contribution as a co-author, I will be glad to distribute your views to the updated list of co-authors for a balanced response. We would ask for your consent on this open bottom-up policy.

Phase 4: We organize a MitoEAGLE session linked to our series of reports at the MiPconference Nov 2017 in Hradec Kralove in close association with the MiPsociety (where you hopefully will attend) and at EBEC 2018 in Budapest.

» http://www.mitoeagle.org/index.php/MiP2017_Hradec_Kralove_CZ

I thank you in advance for your feedback.

With best wishes,

Erich Gnaiger

Chair Mitochondrial Physiology Society - <http://www.mitophysiology.org>

Chair COST Action MitoEAGLE - <http://www.mitoeagle.org>

Medical University of Innsbruck, Austria

97	Contents
98	1. Introduction
99	2. Respiratory coupling states in mitochondrial preparations
100	Mitochondrial preparations
101	2.1. <i>Three coupling states of mitochondrial preparations and residual oxygen consumption</i>
102	Coupling control states and respiratory capacities
103	Kinetic control
104	Phosphorylation, P _o
105	LEAK, OXPHOS, ET, ROX
106	2.2. <i>Coupling states and respiratory rates</i>
107	2.3. <i>Classical terminology for isolated mitochondria</i>
108	States 1-5
109	3. The protonmotive force and proton flux
110	3.1. <i>Electric and chemical partial forces versus electrical and chemical units</i>
111	Faraday constant
112	Electrical part of the protonmotive force
113	Chemical part of the protonmotive force
114	3.2. <i>Definitions</i>
115	Control and regulation
116	Respiratory control and response
117	Respiratory coupling control
118	Pathway control states
119	The steady-state
120	3.3. <i>Forces and fluxes in physics and irreversible thermodynamics</i>
121	Vectorial and scalar forces, and fluxes
122	Coupling
123	Coupled versus bound processes
124	4. Normalization: fluxes and flows
125	4.1. <i>Flux per chamber volume</i>
126	4.2. <i>System-specific and sample-specific normalization</i>
127	Extensive quantities
128	Size-specific quantities
129	Molar quantities
130	Flow per system, I
131	Size-specific flux, J
132	Sample concentration, C_{mX}
133	Mass-specific flux, J_{mX,O_2}
134	Number concentration, C_{NX}
135	Flow per sample entity, I_{X,O_2}
136	4.3. <i>Normalization for mitochondrial content</i>
137	Mitochondrial concentration, C_{mte} , and mitochondrial markers
138	Mitochondria-specific flux, J_{mte,O_2}
139	4.4. <i>Conversion: units and normalization</i>
140	4.5. <i>Conversion: oxygen, proton and ATP flux</i>
141	5. Conclusions
142	6. References
143	

144 **Abstract**

145 Clarity of concept and consistency of nomenclature are key trademarks of a research field.
146 These trademarks facilitate effective transdisciplinary communication, education, and
147 ultimately further discovery. As the knowledge base and importance of mitochondrial
148 physiology to human health expand, the necessity for harmonizing nomenclature concerning
149 mitochondrial respiratory states and rates has become increasingly apparent. Peter Mitchell's
150 concept of the protonmotive force establishes the links between electrical and chemical
151 components of energy transformation and coupling in oxidative phosphorylation. This unifying
152 concept provides the framework for developing a consistent nomenclature for mitochondrial
153 physiology and bioenergetics. Herein, we follow IUPAC guidelines on general terms of
154 physical chemistry, extended by the concepts of open systems and irreversible thermodynamics.
155 We align the nomenclature of classical bioenergetics on respiratory states with a concept-driven
156 constructive terminology to address the meaning of each respiratory state. Furthermore, we
157 suggest uniform standards for the evaluation of respiratory states that will ultimately support
158 the development of databases of mitochondrial respiratory function in species, tissues and cells
159 studied under diverse physiological and experimental conditions. In this position statement, in
160 the frame of COST Action CA15203 MitoEAGLE, we endeavour to provide a balanced view
161 on mitochondrial respiratory control, a fundamental introductory presentation of the concept of
162 the protonmotive force, and a critical discussion on reporting data of mitochondrial respiration
163 in terms of metabolic flows and fluxes.

164

165 *Keywords:* Mitochondrial respiratory control, coupling control, mitochondrial
166 preparations, protonmotive force, chemiosmotic theory, oxidative phosphorylation, OXPHOS,
167 efficiency, electron transfer, ET; proton leak, LEAK, residual oxygen consumption, ROX, State
168 2, State 3, State 4, normalization, flow, flux

169

170

171 **Box 1:**

172

173 **In brief:**174 **mitochondria**175 **and Bioblasts**

- * Does the public expect biologists to understand Darwin's theory of evolution?
- * Do students expect that researchers of bioenergetics can explain Mitchell's theory of chemiosmotic energy transformation?

176 **Mitochondria** were described for the first time in 1857 by Rudolph Albert Kölliker as granular177 structures or 'sarkosomes' *(a reference is needed)*. In 1886 *(a reference is needed)* Richard

178 Altmann called them 'bioblasts' (published 1894). The word 'mitochondrium' (Greek mitos:

179 thread; chondros: granule) was introduced by Carl Benda (1898). Mitochondria are the oxygen

180 consuming electrochemical generators which evolved from endosymbiotic bacteria (Margulis

181 1970; Lane 2005). The bioblasts of Richard Altmann (1894) included not only the mitochondria

182 as presently defined, but also symbiotic and free-living bacteria.

183 We now recognize mitochondria as dynamic organelles with a double membrane that are

184 contained within eukaryotic cells. The mitochondrial inner membrane (mtIM) shows dynamic

185 tubular to disk-shaped cristae that separate the mitochondrial matrix, *i.e.* the internal

186 mitochondrial compartment, and the intermembrane space; the latter being enclosed by the

187 mitochondrial outer membrane (mtOM). Mitochondria are the structural and functional

188 elemental units of cell respiration. Cell respiration is the consumption of oxygen by electron

189 transfer coupled to electrochemical proton translocation across the mtIM. In the process of

190 oxidative phosphorylation (OXPHOS), the reduction of O₂ is electrochemically coupled to the

191 transformation of energy in the form of adenosine triphosphate (ATP; Mitchell 2011). These

192 powerhouses of the cell contain the machinery of the OXPHOS-pathway, including

193 transmembrane respiratory complexes (*i.e.* proton pumps with FMN, Fe-S and cytochrome *b*,194 *c*, *aa*₃ redox systems); alternative dehydrogenases and oxidases; the coenzyme ubiquinone (Q);

195 ATP synthase; the enzymes of the tricarboxylic acid cycle and the fatty acid oxidation enzymes;

196 transporters of ions, metabolites and co-factors; and mitochondrial kinases related to energy

197 transfer pathways. The mitochondrial proteome comprises over 1,200 proteins

198 (MITOCARTA), mostly encoded by nuclear DNA (nDNA), with a variety of functions, many
199 of which are relatively well known (*e.g.* apoptosis-regulating proteins), while others are still
200 under investigation, or need to be identified (*e.g.* alanine transporter).

201 Mitochondria typically maintain several copies of their own genome (hundred to
202 thousands per cell; Cummins 1998), which is almost exclusively maternally inherited (White *et*
203 *al.* 2008) and known as mitochondrial DNA (mtDNA). One exception to strictly maternal
204 inheritance in animals is found in bivalves (Breton *et al.* 2007). mtDNA is 16.5 Kb in length,
205 contains 13 protein-coding genes for subunits of the transmembrane respiratory Complexes CI,
206 CIII, CIV and ATP synthase, and also encodes 22 tRNAs and the mitochondrial 16S and 12S
207 rRNA. The mitochondrial genome is both regulated and supplemented by nuclear-encoded
208 mitochondrial targeted proteins. Evidence has accumulated that additional gene content is
209 encoded in the mitochondrial genome, *e.g.* microRNAs, piRNA, smithRNAs, repeat associated
210 RNA, and even additional proteins (Duarte *et al.* 2014; Lee *et al.* 2015; Cobb *et al.* 2016).

211 The mtIM contains the non-bilayer phospholipid cardiolipin, which is not present in any
212 other eukaryotic cellular membrane. Cardiolipin promotes the formation of respiratory
213 supercomplexes, which are supramolecular assemblies based upon specific, though dynamic,
214 interactions between individual respiratory complexes (Greggio *et al.* 2017; Lenaz *et al.* 2017).
215 Membrane fluidity is an important parameter influencing functional properties of proteins
216 incorporated in the membranes (Waczulikova *et al.* 2007). There is a constant crosstalk between
217 mitochondria and the other cellular components, maintaining cellular mitostasis through
218 regulation at both the transcriptional and post-translational level, and through cell signalling
219 including proteostatic (*e.g.* the ubiquitin-proteasome and autophagy-lysosome pathways) and
220 genome stability modules throughout the cell cycle or even cell death, contributing to
221 homeostatic regulation in response to varying energy demands and stress (Quiros *et al.* 2016).
222 In addition to mitochondrial movement along the microtubules, mitochondrial morphology can
223 change in response to the energy requirements of the cell via processes known as fusion and

224 fission, through which mitochondria can communicate within a network, and in response to
225 intracellular stress factors causing swelling and ultimately permeability transition.

226 Mitochondrial dysfunction is associated with a wide variety of genetic and degenerative
227 diseases. Robust mitochondrial function is supported by physical exercise and caloric balance,
228 and is central for sustained metabolic health throughout life. Therefore, a better understanding
229 of mitochondrial physiology will improve our understanding of the etiology of disease, the
230 diagnostic repertoire of mitochondrial medicine, with a focus on protective medicine, lifestyle
231 and healthy aging.

232 Abbreviation: mt, as generally used in mtDNA. Mitochondrion is singular and
233 mitochondria is plural.

234 *‘For the physiologist, mitochondria afforded the first opportunity for an experimental*
235 *approach to structure-function relationships, in particular those involved in active transport,*
236 *vectorial metabolism, and metabolic control mechanisms on a subcellular level’ (Ernster and*
237 *Schatz 1981).*

238

239 **1. Introduction**

240 Mitochondria are the powerhouses of the cell with numerous physiological, molecular,
241 and genetic functions (**Box 1**). Every study of mitochondrial function and disease is faced with
242 **E**volution, **A**ge, **G**ender and sex, **L**ifestyle, and **E**nvironment (EAGLE) as essential background
243 conditions intrinsic to the individual patient or subject, cohort, species, tissue and to some extent
244 even cell line. As a large and highly coordinated group of laboratories and researchers, the
245 mission of the global MitoEAGLE Network is to generate the necessary scale, type, and quality
246 of consistent data sets and conditions to address this intrinsic complexity. Harmonization of
247 experimental protocols and implementation of a quality control and data management system
248 is required to interrelate results gathered across a spectrum of studies and to generate a
249 rigorously monitored database focused on mitochondrial respiratory function. In this way,

250 researchers within the same and across different disciplines will be positioned to compare their
251 findings to an agreed upon set of clearly defined and accepted international standards.

252 Reliability and comparability of quantitative results depend on the accuracy of
253 measurements under strictly-defined conditions. A conceptually defined framework is also
254 required to warrant meaningful interpretation and comparability of experimental outcomes
255 carried out by research groups at different institutes. With an emphasis on quality of research,
256 collected data can be useful far beyond the specific question of a particular experiment.
257 Enabling meta-analytic studies is the most economic way of providing robust answers to
258 biological questions (Cooper *et al.* 2009). Vague or ambiguous jargon can lead to confusion
259 and may relegate valuable signals to wasteful noise. For this reason, measured values must be
260 expressed in standardized units for each parameter used to define mitochondrial respiratory
261 function. Standardization of nomenclature and definition of technical terms is essential to
262 improve the awareness of the intricate meaning of a divergent scientific vocabulary. The focus
263 on the protonmotive force, coupling states, and fluxes through metabolic pathways of aerobic
264 energy transformation in mitochondrial preparations is a first step in the attempt to generate a
265 harmonized and conceptually-oriented nomenclature in bioenergetics and mitochondrial
266 physiology. Coupling states of intact cells and respiratory control by fuel substrates and specific
267 inhibitors of respiratory enzymes will be reviewed in subsequent communications.

268

269 **2. Respiratory coupling states in mitochondrial preparations**

270 *‘Every professional group develops its own technical jargon for talking about*
271 *matters of critical concern ... People who know a word can share that idea with*
272 *other members of their group, and a shared vocabulary is part of the glue that holds*
273 *people together and allows them to create a shared culture’ (Miller 1991).*

274

275 **Mitochondrial preparations** are defined as either isolated mitochondria, or tissue and
276 cellular preparations in which the barrier function of the plasma membrane is disrupted. The
277 plasma membrane separates the cytosol, nucleus, and organelles (the intracellular
278 compartment) from the environment of the cell. The plasma membrane consists of a lipid
279 bilayer, embedded proteins, and attached organic molecules that collectively control the
280 selective permeability of ions, organic molecules, and particles across the cell boundary. The
281 intact plasma membrane, therefore, prevents the passage of many water-soluble mitochondrial
282 substrates, such as succinate or adenosine diphosphate (ADP), that are required for the analysis
283 of respiratory capacity at kinetically-saturating concentrations, thus limiting the scope of
284 investigations into mitochondrial respiratory function in intact cells. The cholesterol content of
285 the plasma membrane is high compared to mitochondrial membranes. Therefore, mild
286 detergents, such as digitonin and saponin, can be applied to selectively permeabilize the plasma
287 membrane by interaction with cholesterol and allow free exchange of cytosolic components
288 with ions and organic molecules of the immediate cell environment, while maintaining the
289 integrity and localization of organelles, cytoskeleton, and the nucleus. Application of optimum
290 concentrations of these mild detergents leads to the complete loss of cell viability, tested by
291 nuclear staining, while mitochondrial function remains intact, as shown by an unaltered
292 respiration rate of isolated mitochondria after the addition of such low concentrations of digitonin
293 and saponin. In addition to mechanical permeabilization during homogenization of fresh tissue,
294 saponin may be applied to ensure permeabilization of all cells. Crude homogenate and cells
295 permeabilized in the respiration chamber contain all components of the cell at highly diluted
296 concentrations. All mitochondria are retained in chemically-permeabilized mitochondrial
297 preparations and crude tissue homogenates. In the preparation of isolated mitochondria, the
298 cells or tissues are homogenized, and the mitochondria are separated from other cell fractions
299 and purified by differential centrifugation, entailing the loss of a significant fraction of

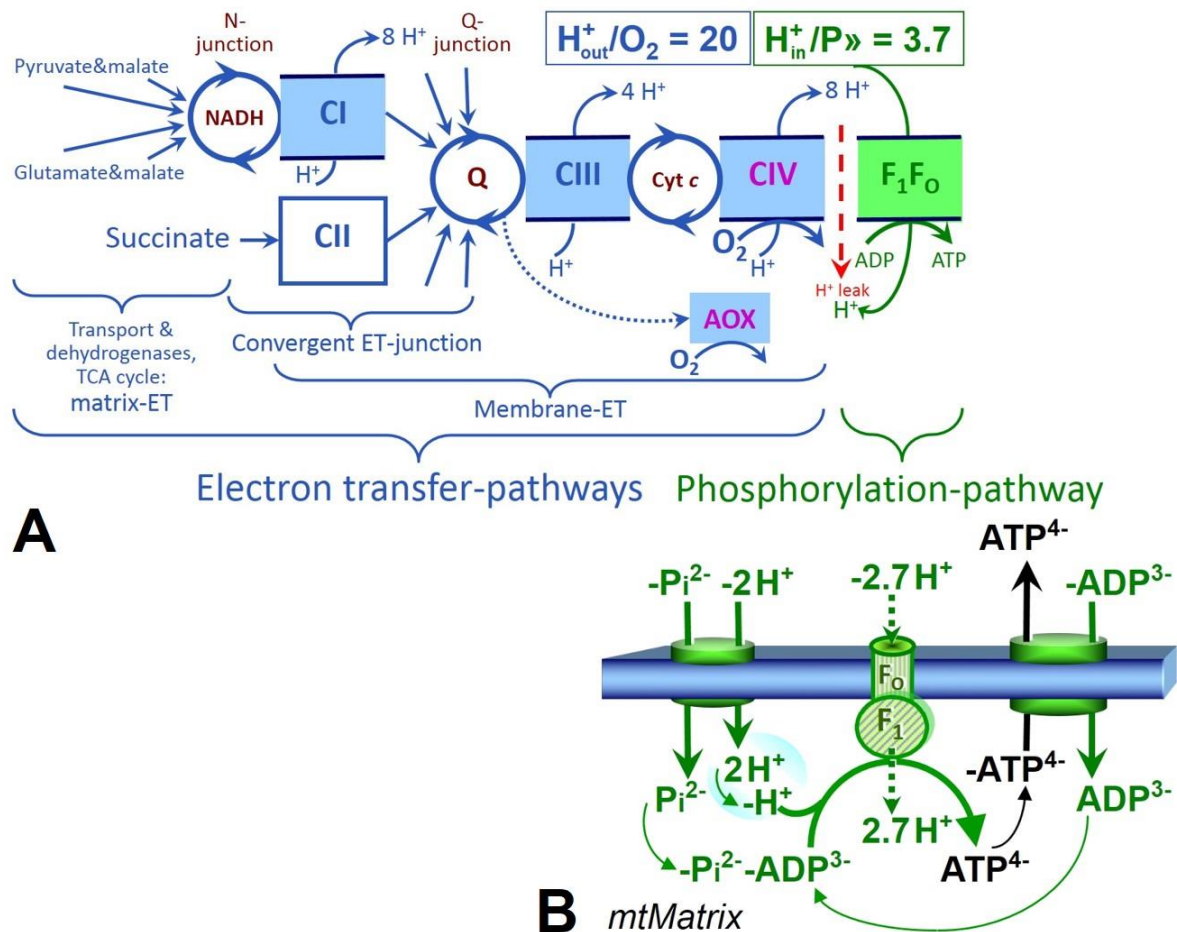
300 mitochondria. The term mitochondrial preparation does not include further fractionation of
301 mitochondrial components, as well as submitochondrial particles.

302

303 *2.1. Three coupling states of mitochondrial preparations and residual oxygen consumption*

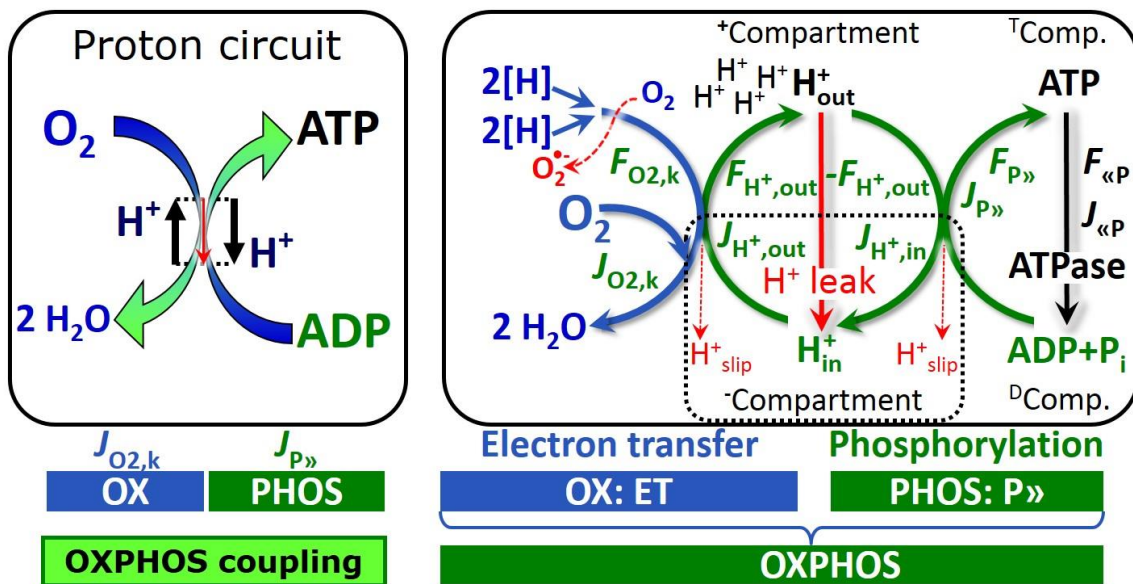
304 **Respiratory capacities in coupling control states:** To extend the classical nomenclature
305 on mitochondrial coupling states (Section 2.4) by a concept-driven terminology that
306 incorporates explicit information on the nature of the respiratory states, the terminology must
307 be general and not restricted to any particular experimental protocol or mitochondrial
308 preparation (Gnaiger 2009). We focus primarily on the conceptual ‘why’, along with
309 clarification of the experimental ‘how’. In the following section, the concept-driven
310 terminology is explained and coupling states are defined. We define respiratory capacities,
311 comparable to channel capacity in information theory (Schneider 2006), as the upper bound of
312 the rate of respiration measured in defined coupling and electron transfer-pathway (ET-
313 pathway) control states. To provide a diagnostic reference for respiratory capacities of core
314 energy metabolism, the capacity of *oxidative phosphorylation*, OXPHOS, is measured at
315 kinetically-saturating concentrations of ADP and inorganic phosphate, P_i . The *oxidative* ET-
316 capacity reveals the limitation of OXPHOS-capacity mediated by the *phosphorylation-*
317 *pathway*. The ET- and phosphorylation-pathways comprise coupled segments of the OXPHOS-
318 pathway. ET-capacity is measured as noncoupled respiration by application of *external*
319 *uncouplers*. The contribution of *intrinsically uncoupled* oxygen consumption is most easily
320 studied in the absence of ADP, *i.e.* by not stimulating phosphorylation, or by inhibition of the
321 phosphorylation-pathway. The corresponding states are collectively classified as LEAK-states,
322 when oxygen consumption compensates mainly for the proton leak (**Table 1**). Different
323 coupling states are induced by (1) adding ADP or P_i , (2) inhibiting the phosphorylation-
324 pathway, and (3) performing uncoupler titrations, while maintaining a defined ET-pathway
325 state with constant fuel substrates and ET inhibitors (**Fig. 1**).

326 **Kinetic control:** Coupling control states are established in the study of mitochondrial
 327 preparations to obtain reference values for various output variables. Physiological conditions *in*
 328 *vivo* may deviate substantially from these experimentally obtained states. Since kinetically-
 329 saturating concentrations, *e.g.* of ADP or oxygen, may not apply to physiological intracellular
 330 conditions, relevant information is obtained in studies of kinetic responses to conditions
 331 intermediate between the LEAK state at zero [ADP] and the OXPHOS-state at saturating
 332 [ADP], or of respiratory capacities in the range between kinetically-saturating [O₂] and anoxia
 333 (Gnaiger 2001).



334
 335 **Fig. 1. The oxidative phosphorylation-pathway, OXPHOS-pathway.** (A) Electron transfer, ET,
 336 coupled to phosphorylation. Multiple convergent ET-pathways are shown from NADH and succinate;
 337 additional arrows indicate electron entry through electron transferring flavoprotein, glycerophosphate
 338 dehydrogenase, dihydro-orotate dehydrogenase, choline dehydrogenase, and sulfide-ubiquinone
 339 oxidoreductase. The branched pathway of oxygen consumption by alternative quinol oxidase (AOX) is

340 indicated by the dotted arrow. The H^+_{out}/O_2 ratio is the outward proton flux from the matrix space divided
 341 by catabolic O_2 flux in the NADH-pathway. The H^+_{in}/P_{\gg} ratio is the inward proton flux from the inter-
 342 membrane space divided by the flux of phosphorylation of ADP to ATP. Due to proton leak and slip
 343 these are not fixed stoichiometries. (B) Phosphorylation-pathway catalyzed by the F_1F_0 ATP synthase,
 344 adenine nucleotide translocase, and inorganic phosphate transporter. The H^+_{in}/P_{\gg} stoichiometry is the
 345 sum of the coupling stoichiometry in the ATP synthase reaction (-2.7 H^+ from the intermembrane space,
 346 2.7 H^+ to the matrix) and the proton balance in the translocation of ADP^{2-} , ATP^{3-} and P_i^{2-} . See Eqs. 3
 347 and 4 for further explanation. Modified from (A) Lemieux *et al.* (2017) and (B) Gnaiger (2014).
 348



349
 350 **Fig. 2. The proton circuit and coupling in oxidative phosphorylation (OXPHOS).** Oxygen flux, $J_{O_2,k}$,
 351 through the catabolic electron transfer-pathway k is coupled to flux through the phosphorylation-pathway
 352 of ADP to ATP, $J_{P_{\gg}}$, by the proton pumps of the ET-pathway, pushing the outward proton flux, $J_{H^+,out}$,
 353 and generating the output protonmotive force, $F_{H^+,out}$. ATP synthase is coupled to inward proton flux,
 354 $J_{H^+,in}$, to phosphorylate $ADP + P_i$ to ATP, driven by the input protonmotive force, $F_{H^+,in} = -F_{H^+,out}$. $2[H]$
 355 indicates the reduced hydrogen equivalents of fuel substrates that provide the chemical input force, $F_{O_2,k}$
 356 $[kJ/mol O_2]$, of the catabolic reaction k with oxygen (Gibbs energy of reaction per mole O_2 consumed in
 357 reaction k), typically in the range of -460 to -480 kJ/mol. The output force is given by the phosphorylation
 358 potential difference (ADP phosphorylated to ATP), $F_{P_{\gg}}$, which varies *in vivo* ranging from about 48 to 62
 359 kJ/mol under physiological conditions (Gnaiger 1993a). Fluxes, J_B , and forces, F_B , are expressed in
 360 either chemical units, $[mol \cdot s^{-1} \cdot m^{-3}]$ and $[J \cdot mol^{-1}]$ respectively, or electrical units, $[C \cdot s^{-1} \cdot m^{-3}]$ and $[J \cdot C^{-1}]$

361 respectively, per volume, V [m^3], of the system. The system defined by the boundaries shown as a full
 362 black line is not a black box, but is analysed as a compartmental system. The negative compartment
 363 ($\bar{\text{C}}$ Compartment, enclosed by the dotted line) is the matrix space, separated from the positive
 364 compartment (^+C Compartment) by the mtIM. ADP+ P_i and ATP are the substrate- and product-
 365 compartments (scalar ADP and ATP compartments, $^{\text{D}}$ Comp. and $^{\text{T}}$ Comp.), respectively. Chemical
 366 potentials of all substrates and products involved in the scalar reactions are measured in the
 367 ^+C Compartment for calculation of the scalar forces $F_{\text{O}_2, \text{k}}$ and $F_{\text{P}\gg} = -F_{\ll\text{P}}$ (**Box 2**). Modified from Gnaiger
 368 (2014).

369

370 **Phosphorylation, $\text{P}\gg$:** *Phosphorylation* in the context of OXPHOS is defined as
 371 phosphorylation of ADP to ATP. On the other hand, the term phosphorylation is used generally
 372 in many different contexts, *e.g.* protein phosphorylation. This justifies consideration of a
 373 symbol more discriminating and specific than P as used in the P/O ratio (phosphate to atomic
 374 oxygen ratio; $\text{O} = 0.5 \text{O}_2$), where P indicates phosphorylation of ADP to ATP or GDP to GTP.
 375 We propose the symbol $\text{P}\gg$ for the endergonic direction of phosphorylation $\text{ADP}\rightarrow\text{ATP}$, and
 376 likewise the symbol $\ll\text{P}$ for the corresponding exergonic hydrolysis $\text{ATP}\rightarrow\text{ADP}$ (**Fig. 2; Box**
 377 **3**). ATP synthase is the proton pump of the phosphorylation-pathway (**Fig. 1B**). $\text{P}\gg$ may also
 378 involve substrate-level phosphorylation as part of the tricarboxylic acid cycle (succinyl-CoA
 379 ligase) and phosphorylation of ADP catalyzed by phosphoenolpyruvate carboxykinase,
 380 adenylate kinase, creatine kinase, hexokinase and nucleoside diphosphate kinase (NDPK).
 381 Kinase cycles are involved in intracellular energy transfer and signal transduction for regulation
 382 of energy flux. In isolated mammalian mitochondria ATP production catalyzed by adenylate
 383 kinase, $2\text{ADP} \leftrightarrow \text{ATP} + \text{AMP}$, proceeds without fuel substrates in the presence of ADP
 384 (Komlódi and Tretter 2017). $J_{\text{P}\gg}/J_{\text{O}_2, \text{k}}$ ($\text{P}\gg/\text{O}_2$) is two times the ‘P/O’ ratio of classical
 385 bioenergetics. The effective $\text{P}\gg/\text{O}_2$ ratio is diminished by: (1) the proton leak across the mtIM
 386 from low pH in the ^+C Compartment to high pH in the $\bar{\text{C}}$ Compartment; (2) cycling of other cations;

387 (3) proton slip in the proton pumps when a proton effectively is not pumped; and (4) electron
 388 leak in the univalent reduction of oxygen (O_2 ; dioxygen) to superoxide anion radical ($O_2^{\bullet-}$).

389

390 **Table 1. Coupling states and residual oxygen consumption in mitochondrial**
 391 **preparations in relation to respiration- and phosphorylation-rate, $J_{O_2,k}$ and $J_{P_{\gg}}$,**
 392 **and protonmotive force, $F_{H^+,out}$.** Coupling states are established at kinetically-
 393 saturating concentrations of fuel substrates and O_2 .

State	$J_{O_2,k}$	$J_{P_{\gg}}$	$F_{H^+,out}$	Inducing factors	Limiting factors
LEAK	L ; low proton leak-dependent respiration	0	max.	Proton leak, slip, and cation cycling	$J_{P_{\gg}} = 0$: (1) without ADP, L_N ; (2) max. ATP/ADP ratio, L_T ; or (3) inhibition of the phosphorylation-pathway, L_{Omy}
OXPHOS	P ; high ADP-stimulated respiration	max.	high	Kinetically-saturating [ADP] and $[P_i]$	$J_{P_{\gg}}$ by phosphorylation-pathway; or $J_{O_2,k}$ by ET-capacity
ET	E ; max. noncoupled respiration	0	low	Optimal external uncoupler concentration for max. oxygen flux	$J_{O_2,k}$ by ET-capacity
ROX	R_{ox} ; min. residual O_2 consumption	0	0	$J_{O_2,R_{ox}}$ in non-ET-pathway oxidation reactions	Full inhibition of ET-pathway or absence of fuel substrates

394

395

396 **LEAK-state (Fig. 3):** The
 397 LEAK-state is defined as a state
 398 of mitochondrial respiration
 399 when O_2 flux mainly
 400 compensates for the proton leak
 401 in the absence of ATP synthesis,

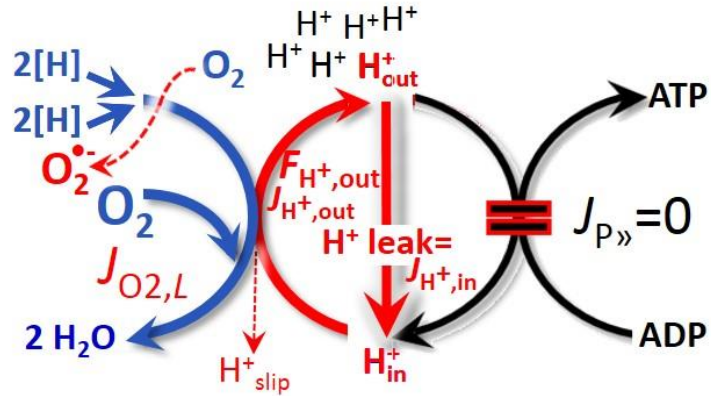


Fig. 3. LEAK-state: Phosphorylation is arrested, $J_{P\gg} = 0$, and oxygen flux, $J_{O_2,L}$, is controlled mainly by the proton leak, which equals $J_{H^+,in}$, at maximum protonmotive force, $F_{H^+,out}$ (See also Fig. 2).

402 at kinetically-saturating
 403 concentrations of O_2 and
 404 respiratory substrates. LEAK-
 405 respiration is measured to obtain
 406 an indirect estimate of *intrinsic uncoupling* without addition of any experimental uncoupler: (1)
 407 in the absence of adenylates; (2) after depletion of ADP at maximum ATP/ADP ratio; or (3)
 408 after inhibition of the phosphorylation-pathway by inhibitors of ATP synthase, such as
 409 oligomycin, or adenine nucleotide translocase, such as carboxyatractyloside.

410

411 **Table 2. Distinction of terms related to coupling.**

Term	Respiration	$P\gg/O_2$	Note
Fully coupled	$P - L$	max.	OXPPOS-capacity corrected for LEAK-respiration (Fig. 6)
Well-coupled	P	High	Phosphorylating respiration with a variable intrinsic LEAK component (Fig. 4)
Loosely coupled	up to E	Low	Inducibly uncoupled by UCPI or Ca^{2+} cycling
Dyscoupled	P	Low	Pathologically, toxicologically, environmentally increased uncoupling, mitochondrial dysfunction
Uncoupled and decoupled	L	0	Non-phosphorylating intrinsic LEAK-respiration without added protonophore (Fig. 3)
Noncoupled	E	0	Non-phosphorylating respiration stimulated to maximum flux at optimum exogenous uncoupler concentration (Fig. 5)

412

413 **Proton leak:** Proton leak is the *uncoupled* process in which protons are translocated
414 across the mtIM in the dissipative direction of the downhill protonmotive force without
415 coupling to phosphorylation (**Fig. 3**). The proton leak flux depends on the protonmotive force,
416 is a property of the mtIM, may be enhanced due to possible contaminations by free fatty acids,
417 and is physiologically controlled. In particular, inducible uncoupling mediated by uncoupling
418 protein 1 (UCP1) is physiologically controlled, *e.g.*, in brown adipose tissue. UCP1 is a proton
419 channel of the mtIM facilitating the conductance of protons across the mtIM (Klingenberg
420 2017). As a consequence of this effective short-circuit, the protonmotive force diminishes,
421 resulting in stimulation of electron transfer to oxygen and heat dissipation without
422 phosphorylation of ADP. Mitochondrial injuries may lead to *dyscoupling* as a pathological or
423 toxicological cause of *uncoupled* respiration, *e.g.*, as a consequence of opening the permeability
424 transition pore. Dyscoupled respiration is distinguished from the experimentally induced
425 *noncoupled* respiration in the ET-state. Under physiological conditions, the proton leak is the
426 dominant contributor to the overall leak current (Dufour *et al.* 1996).

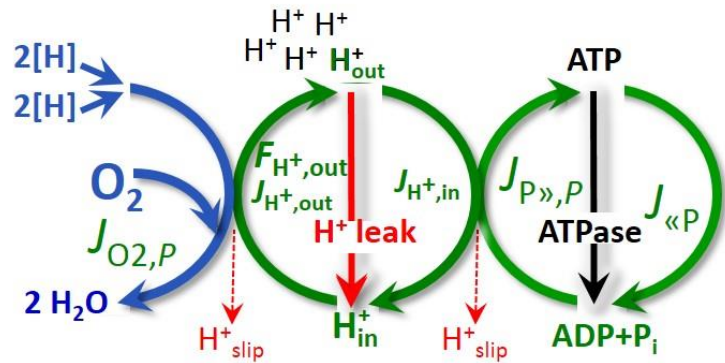
427 **Proton slip:** Proton slip is the *decoupled* process in which protons are only partially
428 translocated by a proton pump of the ET-pathways and slip back to the original compartment
429 (Dufour *et al.* 1996). Proton slip can also happen in association with the ATP-synthase, in which
430 case the proton slips downhill across the membrane to the matrix without contributing to ATP
431 synthesis. In each case, proton slip is a property of the proton pump and increases with the
432 turnover rate of the pump.

433 **Cation cycling:** Proton leak is a leak current of protons. There can be other cation
434 contributors to leak current including calcium and probably magnesium. Calcium current is
435 balanced by mitochondrial Na/Ca exchange, which is balanced by Na/H exchange or K/H
436 exchange. This is another effective uncoupling mechanism different from proton leak and slip.

437 Small differences of terms, *e.g.*, uncoupled, noncoupled, are easily overlooked and may
 438 be erroneously perceived as identical. Even with an attempt at rigorous definition, the common
 439 use of such terms may remain vague (Table 2).

440 **OXPHOS-state** (Fig. 4):

441 The OXPHOS-state is defined as
 442 the respiratory state with
 443 kinetically-saturating
 444 concentrations of O_2 , respiratory
 445 and phosphorylation substrates,
 446 and absence of exogenous
 447 uncoupler, which provides an
 448 estimate of the maximal
 449 respiratory capacity in the



450 **Fig. 4. OXPHOS-state:** Phosphorylation, $J_{P \gg}$, is stimulated
 451 by kinetically-saturating [ADP] and inorganic phosphate,
 452 [P_i], and is supported by a high protonmotive force, $F_{H^+,out}$.
 453 O_2 flux, $J_{O_2,P}$, is well-coupled at a $P \gg / O_2$ ratio of $J_{P \gg, P} / J_{O_2, P}$
 454 (See also Fig. 2).

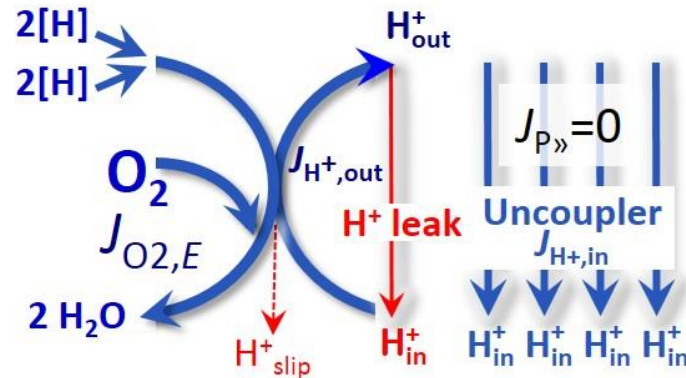
450 OXPHOS-state for any given ET-pathway state. Respiratory capacities at kinetically-saturating
 451 substrate concentrations provide reference values or upper limits of performance, aiming at the
 452 generation of data sets for comparative purposes. Any effects of substrate kinetics are thus
 453 separated from reporting actual mitochondrial capacity for oxidation during well-coupled
 454 respiration, against which physiological activities can be evaluated.

455 As discussed previously, 0.2 mM ADP does not fully saturate flux in isolated
 456 mitochondria (Gnaiger 2001; Puchowicz *et al.* 2004); greater ADP concentration is required,
 457 particularly in permeabilized muscle fibres and cardiomyocytes, to overcome limitations by
 458 intracellular diffusion and by the reduced conductance of the mitochondrial outer membrane,
 459 mtOM (Jepihhina *et al.* 2011, Illaste *et al.* 2012, Simson *et al.* 2016) either through interaction
 460 with tubulin (Rostovtseva *et al.* 2008) or other intracellular structures (Birkedal *et al.* 2014). In
 461 permeabilized muscle fibre bundles of high respiratory capacity, the apparent K_m for ADP
 462 increases up to 0.5 mM (Saks *et al.* 1998), indicating that >90% saturation is reached only at

463 >5 mM ADP. Similar ADP concentrations are also required for accurate determination of
 464 OXPHOS-capacity in human clinical cancer samples and permeabilized cells (Klepinin *et al.*
 465 2016; Koit *et al.* 2017). Whereas 2.5 to 5 mM ADP is sufficient to obtain the actual OXPHOS-
 466 capacity in many types of permeabilized cell and tissue preparations, experimental validation
 467 is required in each specific case.

468 Electron transfer-state

469 (Fig. 5): The ET-state is defined
 470 as the *noncoupled* state with
 471 kinetically-saturating
 472 concentrations of O₂, respiratory
 473 substrate and optimum
 474 exogenous uncoupler
 475 concentration for maximum O₂
 476 flux, as an estimate of oxidative



477 **Fig. 5. ET-state:** Noncoupled respiration, $J_{O_2,E}$, is maximum
 478 at optimum exogenous uncoupler concentration and
 479 phosphorylation is zero, $J_{P,»} = 0$ (See also Fig. 2).

477 ET-capacity. Inhibition of respiration is observed at higher than optimum uncoupler
 478 concentrations. As a consequence of the nearly collapsed protonmotive force, the driving force
 479 is insufficient for phosphorylation and $J_{P,»} = 0$.

480 Besides the three fundamental coupling states of mitochondrial preparations, the
 481 following respiratory state also is relevant to assess respiratory function:

482 **ROX:** Residual oxygen consumption (ROX) is defined as O₂ consumption due to
 483 oxidative side reactions remaining after inhibition of ET with rotenone, malonic acid and
 484 antimycin A. Cyanide and azide not only inhibit CIV but several peroxidases which might be
 485 involved in ROX. ROX is not a coupling state but represents a baseline that is used to correct
 486 mitochondrial respiration in defined coupling states. ROX is not necessarily equivalent to non-
 487 mitochondrial respiration, considering oxygen-consuming reactions in mitochondria not related
 488 to ET, such as oxygen consumption in reactions catalyzed by monoamine oxidases (type A and

489 B), monooxygenases (cytochrome P450 monooxygenases), dioxygenase (sulfur dioxygenase
 490 and trimethyllysine dioxygenase), several hydroxylases, and more. Mitochondrial preparations,
 491 especially those obtained from liver, are contaminated by peroxisomes. This fact makes the
 492 exact determination of mitochondrial oxygen consumption and mitochondria-associated
 493 generation of reactive oxygen species complicated (Schönfeld *et al.* 2009). The dependence of
 494 ROX-linked oxygen consumption needs to be studied in detail with respect to non-ET enzyme
 495 activities, availability of specific substrates, oxygen concentration, and electron leakage leading
 496 to the formation of reactive oxygen species.

497

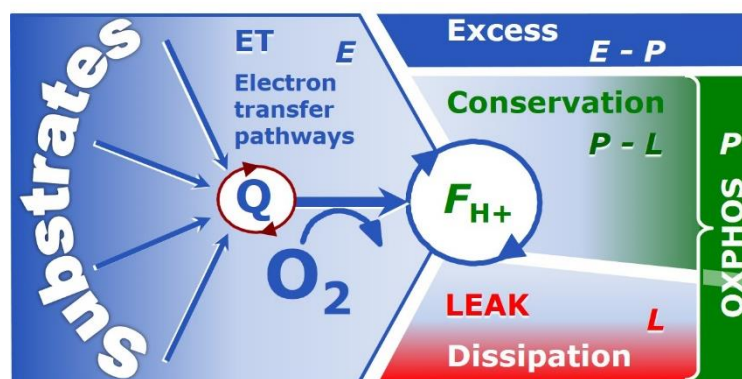
498 2.2. Coupling states and respiratory rates

499 It is important to distinguish metabolic pathways from metabolic states and the
 500 corresponding metabolic rates; for example: ET-pathways (Fig. 6), ET-state (Fig. 5), and ET-
 501 capacity, E , respectively (Table 1). The protonmotive force is *high* in the OXPHOS-state when
 502 it drives phosphorylation, *maximum* in the LEAK-state of coupled mitochondria, driven by
 503 LEAK-respiration at a minimum back flux of protons to the matrix side, and *very low* in the
 504 ET-state when uncouplers short-circuit the proton cycle (Table 1).

505

506 **Fig. 6. Four-compartment model**
 507 **of oxidative phosphorylation.**

508 Respiratory states (ET, OXPHOS,
 509 LEAK) and corresponding rates (E ,
 510 P , L) are connected by the
 511 protonmotive force, $F_{H+,out}$. Electron
 512 transfer-capacity, E , is partitioned



513 into (1) dissipative LEAK-respiration, L , when the capacity to perform work is irreversibly lost, (2) net
 514 OXPHOS-capacity, $P-L$, with partial conservation of the capacity to perform work, and (3) the excess
 515 capacity, $E-P$. Modified from Gnaiger (2014).

516

517 The three coupling states, ET, LEAK and OXPHOS, are presented in a schematic context
518 with the corresponding respiratory rates, abbreviated as E , L and P , respectively (Fig. 6). This
519 clarifies that E may exceed or be equal to P , but E cannot theoretically be lower than P . $E < P$
520 must be discounted as an artefact, which may be caused experimentally by: (1) loss of oxidative
521 capacity during the time course of the respirometric assay, since E is measured subsequently to
522 P ; (2) using insufficient uncoupler concentrations; (3) using high uncoupler concentrations which
523 inhibit ET (Gnaiger 2008); (4) high oligomycin concentrations applied for measurement of L
524 before titrations of uncoupler, when oligomycin exerts an inhibitory effect on E . On the other
525 hand, the excess ET-capacity is overestimated if non-saturating $[P_i]$ or $[ADP]$ are used (see
526 State 3 in the next section).

527 $E > P$ is observed in many types of mitochondria, varying between species, tissues and
528 cell types. It is the excess ET-capacity pushing the phosphorylation-flux (Fig. 1B) to the limit
529 of its *capacity of utilizing* the protonmotive force. Within any type of mitochondria, the
530 magnitude of $E > P$ depends on (1) the pathway control state with single or multiple electron
531 input into the Q-junction and involvement of three or fewer coupling sites determining the
532 H^+_{out}/O_2 *coupling stoichiometry* (Fig. 1A); and (2) the *biochemical coupling efficiency*
533 expressed as $(E-L)/E$, since an increase of L causes P to increase towards the limit of E . The
534 *excess E-P capacity*, $E-P$, therefore, provides a sensitive diagnostic indicator of specific injuries
535 of the phosphorylation-pathway, under conditions when E remains constant but P declines
536 relative to controls (Fig. 6). Substrate cocktails supporting simultaneous convergent electron
537 transfer to the Q-junction for reconstitution of tricarboxylic acid cycle (TCA cycle) function
538 establish pathway control states with high ET-capacity, and consequently increase the
539 sensitivity of the $E-P$ assay.

540 When subtracting L from P , the dissipative LEAK component in the OXPHOS-state may
541 be overestimated. This can be avoided by measuring LEAK-respiration in a state when the
542 protonmotive force is adjusted to its slightly lower value in the OXPHOS-state, *e.g.*, by titration

543 of an ET inhibitor. Any turnover-dependent components of proton leak and slip, however, are
 544 underestimated under these conditions (Garlid *et al.* 1993). In general, it is inappropriate to use
 545 the term *ATP production* or *ATP turnover* for the difference of oxygen consumption measured
 546 in states *P* and *L*. The difference *P-L* is the upper limit of the part of OXPHOS-capacity that is
 547 freely available for ATP production (corrected for LEAK-respiration) and is fully coupled to
 548 phosphorylation with a maximum mechanistic stoichiometry (**Fig. 6**).

549

550 2.3. Classical terminology for isolated mitochondria

551 *‘When a code is familiar enough, it ceases appearing like a code; one forgets that*
 552 *there is a decoding mechanism. The message is identical with its meaning’*
 553 (Hofstadter 1979).

554 Chance and Williams (1955; 1956) introduced five classical states of mitochondrial respiration
 555 and cytochrome redox states. **Table 3** shows a protocol with isolated mitochondria in a closed
 556 respirometric chamber, defining a sequence of respiratory states.

557 **Table 3. Metabolic states of mitochondria (Chance and**
 558 **Williams, 1956; Table V).**
 559

State	[O ₂]	ADP level	Substrate level	Respiration rate	Rate-limiting substance
1	>0	low	low	slow	ADP
2	>0	high	~0	slow	substrate
3	>0	high	high	fast	respiratory chain
4	>0	low	high	slow	ADP
5	0	high	high	0	oxygen

560

561 **State 1** is obtained after addition of isolated mitochondria to air-saturated
 562 isoosmotic/isotonic respiration medium containing inorganic phosphate, but no fuel substrates
 563 and no adenylates, *i.e.*, AMP, ADP, ATP.

564 **State 2** is induced by addition of a high concentration of ADP (typically 100 to 300 μ M),
 565 which stimulates respiration transiently on the basis of endogenous fuel substrates and

566 phosphorylates only a small portion of the added ADP. State 2 is then obtained at a low
567 respiratory activity limited by zero endogenous fuel substrate availability (**Table 3**). If addition
568 of specific inhibitors of respiratory complexes, such as rotenone, does not cause a further
569 decline of oxygen consumption, State 2 is equivalent to residual oxygen consumption (See
570 below). If inhibition is observed, undefined endogenous fuel substrates are a confounding factor
571 of pathway control by externally added substrates and inhibitors. In contrast to the original
572 protocol, an alternative sequence of titration steps is frequently applied, in which the alternative
573 State 2 has an entirely different meaning, when this second state is induced by addition of fuel
574 substrate without ADP (LEAK-state; in contrast to State 2 defined in **Table 2** as a ROX state),
575 followed by addition of ADP.

576 **State 3** is the state stimulated by addition of fuel substrates while the ADP concentration
577 is still high (**Table 3**) and supports coupled energy transformation through oxidative
578 phosphorylation. 'High ADP' is a concentration of ADP specifically selected to allow the
579 measurement of State 3 to State 4 transitions of isolated mitochondria in a closed respirometric
580 chamber. Repeated ADP titration re-establishes State 3 at 'high ADP'. Starting at oxygen
581 concentrations near air-saturation (ca. 200 μM O_2 at sea level and 37 °C), the total ADP
582 concentration added must be low enough (typically 100 to 300 μM) to allow phosphorylation
583 to ATP at a coupled oxygen consumption that does not lead to oxygen depletion during the
584 transition to State 4. In contrast, kinetically-saturating ADP concentrations usually are an order
585 of magnitude higher than 'high ADP', *e.g.* 2.5 mM in isolated mitochondria. The abbreviation
586 State 3u is frequently used in bioenergetics, to indicate the state of respiration after titration of
587 an uncoupler, without sufficient emphasis on the fundamental difference between OXPHOS-
588 capacity (*well-coupled* with an *endogenous* uncoupled component) and ET-capacity
589 (*noncoupled*).

590 **State 4** is a LEAK-state that is obtained only if the mitochondrial preparation is intact
591 and well-coupled. Depletion of ADP by phosphorylation to ATP leads to a decline in oxygen

592 consumption in the transition from State 3 to State 4. Under these conditions, a maximum
 593 protonmotive force and high ATP/ADP ratio are maintained, and the P_{\gg}/O_2 ratio can be
 594 calculated. State 4 respiration, L_T (**Table 1**), reflects intrinsic proton leak and intrinsic ATP
 595 hydrolysis activity. Oxygen consumption in State 4 is an overestimation of LEAK-respiration
 596 if the contaminating ATP hydrolysis activity recycles some ATP to ADP, $J_{\ll P}$, which stimulates
 597 respiration coupled to phosphorylation, $J_{P\gg} > 0$. This can be tested by inhibition of the
 598 phosphorylation-pathway using oligomycin, ensuring that $J_{P\gg} = 0$ (State 4o). Alternatively,
 599 sequential ADP titrations re-establish State 3, followed by State 3 to State 4 transitions while
 600 sufficient oxygen is available. However, anoxia may be reached before exhaustion of ADP
 601 (State 5).

602 **State 5** is the state after exhaustion of oxygen in a closed respirometric chamber.
 603 Diffusion of oxygen from the surroundings into the aqueous solution may be a confounding
 604 factor preventing complete anoxia (Gnaiger 2001). Chance and Williams (1955) provide an
 605 alternative definition of State 5, which gives it the meaning of ROX: ‘State 5 may be obtained
 606 by antimycin A treatment or by anaerobiosis’.

607 In **Table 3**, only States 3 and 4 (and ‘State 2’ in the alternative protocol without ADP;
 608 not included in the table) are coupling control states, with the restriction that O_2 flux in State 3
 609 may be limited kinetically by non-saturating ADP concentrations (**Table 1**).

610

611 **3. The protonmotive force and proton flux**

612 *3.1. Electric and chemical partial forces versus electrical and chemical units*

613 The protonmotive force across the mtIM (Mitchell and Moyle 1967) was introduced most
 614 beautifully in the *Grey Book 1966* (see Mitchell 2011),

$$615 \quad \Delta p_{H^+} = \Delta \Psi + \Delta \mu_{H^+}/F \quad (\text{Eq. 1})$$

616 The protonmotive force consists of two partial forces: (I) The electrical part, $\Delta \Psi$, is the
 617 difference of charge (electric potential difference), is not specific for H^+ , and can, therefore, be

618 measured by the distribution of other cations between the positive and negative compartment
 619 (**Fig. 2**). (2) The chemical part, $\Delta\mu_{H^+}$, is the chemical potential difference in H^+ , is proportional
 620 to the pH difference, and incorporates the Faraday constant (**Table 4**).

621
 622 **Table 4. Protonmotive force and flux matrix.** Columns: The protonmotive force is
 623 the sum of *partial isomorphic forces*, F_{el} and $F_{H^+,d}$. Rows: Electrical and chemical units
 624 (isomorphic format e and n). The Faraday constant, F , converts protonmotive force
 625 and flux from *format e* to n . In contrast to force (state), the conjugated flux (rate) cannot
 626 be partitioned.
 627

State	Force		electric	+ chem.	Unit	Notes	
Protonmotive force, e	Δp_{H^+}	=	$\Delta\Psi$	+ $\Delta\mu_{H^+}/F$	$J\cdot C^{-1}$	$1e$	
Chemiosmotic potential, n	$\Delta\tilde{\mu}_{H^+}$	=	$\Delta\Psi\cdot F$	+ $\Delta\mu_{H^+}$	$J\cdot mol^{-1}$	$1n$	
State	Isomorphic force		$F_{H^+,out/i}$	e_{out}	+ $H^+_{out,d}$		
Electric charge, e	$F_{H^+,out/e}$	=	$F_{el,out/e}$	+ $F_{H^+,out,d/e}$	$J\cdot C^{-1}$	$2e$	
Amount of substance, n	$F_{H^+,out/n}$	=	$F_{el,out/n}$	+ $F_{H^+,out,d/n}$	$J\cdot mol^{-1}$	$2n$	
Rate	Isomorphic flux		$J_{H^+,out/i}$	e	or	n	
Electric charge, e	$J_{H^+,out/e}$		$J_{H^+,out/e}$			$C\cdot s^{-1}\cdot m^{-3}$	$3e$
Amount of substance, n	$J_{H^+,out/n}$				$J_{H^+,out/n}$	$mol\cdot s^{-1}\cdot m^{-3}$	$3n$

628
 629 1: The Faraday constant, F , is the product of elementary charge ($e = 1.602177\cdot 10^{-19}\cdot C$) and the
 630 Avogadro (Loschmidt) constant ($N_A = 6.022136\cdot 10^{23}\cdot mol^{-1}$), $F = eN_A = 96,485.3 C/mol$. $\Delta\tilde{\mu}_{H^+}$ is the
 631 chemiosmotic potential difference. $1e$ and $1n$ are the classical representations of $2e$ and $2n$.
 632 2: The protonmotive force is $F_{H^+,out}$, expressed either in isomorphic format e or n . $F_{el/e} \equiv \Delta\Psi$ is the partial
 633 protonmotive force (el) acting generally on charged motive molecules (*i.e.* ions that are displaceable
 634 across the mtIM). In contrast, $F_{H^+,d/n} \equiv \Delta\mu_{H^+}$ is the partial protonmotive force specific for proton
 635 displacement (H^+_d). The sign of the force is negative for exergonic transformations in which exergy
 636 is lost or dissipated, and positive for endergonic transformations which conserve exergy from a
 637 coupled exergonic process (**Box 3**).

638 3: The sign of the flux depends on the definition of the compartmental direction of the translocation (**Fig.**
 639 **2**). A process is the product of flux and force: $J_{H^+,out/e} \cdot F_{H^+,out/e} = J_{H^+,out/n} \cdot F_{H^+,out/n} = \text{volume-specific power}$
 640 $[\text{J} \cdot \text{s}^{-1} \cdot \text{m}^{-3} = \text{W} \cdot \text{m}^{-3}]$.

641

642 **Faraday constant**, $F = eN_A$ [C/mol] (**Table 4**), enables the conversion between
 643 protonmotive force, $F_{H^+,out/e} \equiv \Delta p_{H^+}$ [J/C], expressed per *motive charge*, e [C], and protonmotive
 644 force or electrochemical potential difference, $F_{H^+,out/n} \equiv \Delta \tilde{\mu}_{H^+} = \Delta p_{H^+} \cdot F$ [J/mol], expressed per
 645 *motive amount of protons*, n [mol]. Proton charge, e , and amount of substance, n , define the
 646 units for the isomorphic formats. Taken together, F converts protonmotive force and flux from
 647 isomorphic format e to n (Eq. 2; see also **Table 4**, Note 2),

$$648 \quad F_{H^+,out/n} = F_{H^+,out/e} \cdot eN_A \quad (\text{Eq. 2.1})$$

$$649 \quad J_{H^+,out/n} = J_{H^+,out/e} / (eN_A) \quad (\text{Eq. 2.2})$$

650 In each format, the protonmotive force is expressed as the sum of two partial forces. The
 651 concept expressed by the complex symbols in Eq. 1 can be explained and visualized more easily
 652 by *partial isomorphic forces* as the components of the protonmotive force:

653 **Electrical part of the protonmotive force:** (1) Isomorph e : $F_{el/e} \equiv \Delta \Psi$ is the electrical
 654 part of the protonmotive force expressed in units joule per coulomb, *i.e.* volt [$\text{V} = \text{J}/\text{C}$]. $F_{el/e}$ is
 655 defined as partial Gibbs energy change per *motive elementary charge*, e [C], not specific for
 656 proton charge (**Table 4**, Note 2e). (2) Isomorph n : $F_{el/n} \equiv \Delta \Psi \cdot F$ is the electric force expressed
 657 in units joule per mole [J/mol], defined as partial Gibbs energy change per *motive amount of*
 658 *charge*, n [mol], not specific for proton charge (**Table 4**, Note 2n).

659 **Chemical part of the protonmotive force:** (1) Isomorph n : $F_{d,H^+/n} \equiv \Delta \mu_{H^+}$ is the chemical
 660 part (diffusion, displacement of H^+) of the protonmotive force expressed in units joule per mole
 661 [J/mol]. $F_{d,H^+/n}$ is defined as partial Gibbs energy change per *motive amount of protons*, n [mol]
 662 (**Table 4**, Note 2n). (2) Isomorph e : $F_{d,H^+/e} \equiv \Delta \mu_{H^+} / F$ is the chemical force expressed in units

663 joule per coulomb [V], defined as partial Gibbs energy change per *motive amount of protons*
 664 *expressed in units of electric charge, e [C], but specific for proton charge (Table 4, Note 2e).*

665 Protonmotive means that there is a potential for the movement of protons, and force is a
 666 measure of the potential for motion. Motion is relative and not absolute (Principle of Galilean
 667 Relativity); likewise there is no absolute potential, but (isomorphic) forces are potential
 668 differences. An electric partial force expressed in the format of electric charge, $F_{el/e}$, of -0.2 V
 669 (Table 5, Note 5e) is equivalent to force in the format of amount, $F_{el,H+/n}$, of $19 \text{ kJ}\cdot\text{mol}^{-1} \text{ H}^+_{out}$
 670 (Note 5n). For a ΔpH of 1 unit, the chemical partial force in the format of amount, $F_{d,H+/n}$,
 671 changes by $5.9 \text{ kJ}\cdot\text{mol}^{-1}$ (Table 5, Note 6n) and chemical force in the format of charge $F_{d,H+/e}$
 672 changes by 0.06 V (Note 6e). Considering a driving force of $-470 \text{ kJ}\cdot\text{mol}^{-1} \text{ O}_2$ for oxidation, the
 673 thermodynamic limit of the $\text{H}^+_{out}/\text{O}_2$ ratio is reached at a value of $470/19 = 24$, compared to a
 674 mechanistic stoichiometry of 20 (Fig. 1).

675

676 3.2. Definitions

677 **Control and regulation:** The terms metabolic *control* and *regulation* are frequently used
 678 synonymously, but are distinguished in metabolic control analysis: ‘We could understand the
 679 regulation as the mechanism that occurs when a system maintains some variable constant over
 680 time, in spite of fluctuations in external conditions (homeostasis of the internal state). On the
 681 other hand, metabolic control is the power to change the state of the metabolism in response to
 682 an external signal’ (Fell 1997). Respiratory control may be induced by experimental control
 683 signals that *exert* an influence on: (1) ATP demand and ADP phosphorylation-rate; (2) fuel
 684 substrate composition, pathway competition; (3) available amounts of substrates and oxygen,
 685 *e.g.*, starvation and hypoxia; (3) the protonmotive force, redox states, flux-force relationships,
 686 coupling and efficiency; (4) Ca^{2+} and other ions including H^+ ; (5) inhibitors, *e.g.*, nitric oxide
 687 or intermediary metabolites, such as oxaloacetate; (6) signalling pathways and regulatory
 688 proteins, *e.g.* insulin resistance, transcription factor HIF-1 or inhibitory factor 1. *Mechanisms*

689 of respiratory control and regulation include adjustments of (1) enzyme activities by allosteric
690 mechanisms and phosphorylation, (2) enzyme content, concentrations of cofactors and
691 conserved moieties (such as adenylates, nicotinamide adenine dinucleotide [NAD⁺/NADH],
692 coenzyme Q, cytochrome *c*); (3) metabolic channeling by supercomplexes; and (4)
693 mitochondrial density (enzyme concentrations and membrane area) and morphology (cristae
694 folding, fission and fusion). (5) Mitochondria are targeted directly by hormones, thereby
695 affecting their energy metabolism (Lee *et al.* 2013; Gerö and Szabo 2016; Price and Dai 2016;
696 Moreno *et al.* 2017). Evolutionary or acquired differences in the genetic and epigenetic basis
697 of mitochondrial function (or dysfunction) between subjects and gene therapy; age; gender,
698 biological sex, and hormone concentrations; life style including exercise and nutrition; and
699 environmental issues including thermal, atmospheric, toxicological and pharmacological
700 factors, exert an influence on all control mechanisms listed above (for reviews, see Brown 1992;
701 Gnaiger 1993a, 2009; 2014; Paradies *et al.* 2014; Morrow *et al.* 2017).

702 **Respiratory control and response:** Lack of control by a metabolic pathway, *e.g.*
703 phosphorylation-pathway, does mean that there will be no response to a variable activating it,
704 *e.g.* [ADP]. However, the reverse is not true as the absence of a response to [ADP] does not
705 exclude the phosphorylation-pathway from having some degree of control. The degree of
706 control of a component of the OXPHOS-pathway on an output variable, such as oxygen flux,
707 will in general be different from the degree of control on other outputs, such as phosphorylation-
708 flux or proton leak flux (**Box 2**). As such, it is necessary to be specific as to which input and
709 output are under consideration (Fell 1997). Therefore, the term respiratory control is elaborated
710 in more detail in the following section.

711 **Respiratory coupling control:** Respiratory control refers to the ability of mitochondria
712 to adjust oxygen consumption in response to external control signals by engaging various
713 mechanisms of control and regulation. Respiratory control is monitored in a mitochondrial
714 preparation under conditions defined as respiratory states. When phosphorylation of ADP to

715 ATP is stimulated or depressed, an increase or decrease is observed in electron flux linked to
716 oxygen consumption in respiratory coupling states of intact mitochondria ('controlled states' in
717 the classical terminology of bioenergetics). Alternatively, coupling of electron transfer with
718 phosphorylation is disengaged by disruption of the integrity of the mtIM or by uncouplers,
719 functioning like a clutch in a mechanical system. The corresponding coupling control state is
720 characterized by high levels of oxygen consumption without control by phosphorylation
721 ('uncontrolled state'). Energetic coupling is defined in **Box 4**. Loss of coupling lowers the
722 efficiency by intrinsic uncoupling and decoupling, or pathological dyscoupling. Such
723 generalized uncoupling is different from switching to mitochondrial pathways that involve
724 fewer than three proton pumps ('coupling sites': Complexes CI, CIII and CIV), bypassing CI
725 through multiple electron entries into the Q-junction (**Fig. 1**). A bypass of CIII and CIV is
726 provided by alternative oxidases, which reduce oxygen without proton translocation.
727 Reprogramming of mitochondrial pathways may be considered as a switch of gears (changing
728 the stoichiometry) rather than uncoupling (loosening the stoichiometry).

729 **Pathway control states** are obtained in mitochondrial preparations by depletion of
730 endogenous substrates and addition to the mitochondrial respiration medium of fuel substrates
731 (CHNO) and specific inhibitors, activating selected mitochondrial pathways (**Fig. 1**). Coupling
732 control states and pathway control states are complementary, since mitochondrial preparations
733 depend on an exogenous supply of pathway-specific fuel substrates and oxygen (Gnaiger 2014).

734

735 **Box 2: Metabolic fluxes and flows: vectorial and scalar**

736 In mitochondrial electron transfer (**Fig. 1**), vectorial transmembrane proton flux is coupled
737 through the proton pumps CI, CIII and CIV to the catabolic flux of scalar reactions, collectively
738 measured as oxygen flux. In **Fig. 2**, the scalar catabolic reaction, k , of oxygen consumption,
739 $J_{O_2,k}$ [$\text{mol}\cdot\text{s}^{-1}\cdot\text{m}^{-3}$], is expressed as oxygen flux per volume, V [m^3], of the instrumental chamber
740 (the system).

741 Fluxes are *vectors*, if they have *spatial* direction in addition to magnitude. A vector flux
 742 (surface-density of flow) is expressed per unit cross-sectional area, A [m^2], perpendicular to the
 743 direction of flux. If *flows*, I , are defined as extensive quantities of the *system*, as vector or scalar
 744 flow, \mathbf{I} or I [$\text{mol}\cdot\text{s}^{-1}$], respectively, then the corresponding vector and scalar *fluxes*, \mathbf{J} , are
 745 obtained as $\mathbf{J} = \mathbf{I}\cdot A^{-1}$ [$\text{mol}\cdot\text{s}^{-1}\cdot\text{m}^{-2}$] and $J = I\cdot V^{-1}$ [$\text{mol}\cdot\text{s}^{-1}\cdot\text{m}^{-3}$], respectively, expressing flux as an
 746 area-specific vector or volume-specific scalar quantity.

747 Vectorial transmembrane proton flux, $J_{\text{H}^+, \text{out}}$, is analyzed in a heterogenous
 748 compartmental system as a quantity with *directional* but not *spatial* information. Translocation
 749 of protons across the mtIM has a defined direction, either from the negative compartment
 750 (matrix space; negative or $\bar{\text{C}}$ Compartment) to the positive compartment (inter-membrane space;
 751 positive or C Compartment) or *vice versa* (**Fig. 2**). The arrows defining the direction of the
 752 translocation between the two compartments may point upwards or downwards, right or left,
 753 without any implication that these are actual directions in space. The ‘upper’ compartment of
 754 the C Compartment is neither above nor below the $\bar{\text{C}}$ Compartment in a spatial sense, but can be
 755 visualized arbitrarily in a figure as the upper compartment (**Fig. 2**). In general, the
 756 *compartmental direction* of vectorial translocation from the $\bar{\text{C}}$ Compartment to the
 757 C Compartment is defined by assigning the initial and final state as *ergodynamic compartments*,
 758 $\text{H}^+_{\text{in}} \rightarrow \text{H}^+_{\text{out}}$, respectively, related to work (erg = work) that must be performed to lift the proton
 759 from a lower to a higher electrochemical potential or from the lower to the higher ergodynamic
 760 compartment (Gnaiger 1993b).

761 In direct analogy to *vectorial* translocation, the direction of a *scalar* chemical reaction, A
 762 $\rightarrow B$, is defined by assigning substrates and products, A and B , as ergodynamic compartments.
 763 O_2 is defined as a substrate in respiratory O_2 consumption, which together with the fuel
 764 substrates comprises the substrate compartment of the catabolic reaction (**Fig. 2**). Volume-
 765 specific scalar O_2 flux is coupled (**Box 4**) to vectorial translocation. In order to establish a
 766 quantitative relation between the coupled fluxes, both $J_{\text{O}_2, \text{k}}$ and $J_{\text{H}^+, \text{out}}$ must be expressed in

767 identical isomorphic units ($[\text{mol}\cdot\text{s}^{-1}\cdot\text{m}^{-3}]$ or $[\text{C}\cdot\text{s}^{-1}\cdot\text{m}^{-3}]$), yielding the $\text{H}^+_{\text{out}}/\text{O}_2$ ratio (**Fig. 1**). The
 768 *vectorial* proton flux in compartmental translocation has *compartmental direction*,
 769 distinguished from a *vector* flux with *spatial direction*. Likewise, the corresponding
 770 protonmotive force is defined as an electrochemical potential *difference* between two
 771 compartments, in contrast to a *gradient* across the membrane or a vector force with defined
 772 spatial direction.

773

774 **The steady-state:** Mitochondria represent a thermodynamically open system functioning
 775 as a biochemical transformation system in non-equilibrium states. State variables (protonmotive
 776 force; redox states) and metabolic fluxes (*rates*) are measured in defined mitochondrial
 777 respiratory *states*. Strictly, steady states can be obtained only in open systems, in which changes
 778 due to *internal* transformations, *e.g.*, O_2 consumption, are instantaneously compensated for by
 779 *external* fluxes *e.g.*, O_2 supply, such that oxygen concentration does not change in the system
 780 (Gnaiger 1993b). Mitochondrial respiratory states monitored in closed systems satisfy the
 781 criteria of pseudo-steady states for limited periods of time, when changes in the system
 782 (concentrations of O_2 , fuel substrates, ADP, P_i , H^+) do not exert significant effects on metabolic
 783 fluxes (respiration, phosphorylation). Such pseudo-steady states require respiratory media with
 784 sufficient buffering capacity and kinetically-saturating concentrations of substrates to be
 785 maintained, and thus depend on the kinetics of the processes under investigation. Proton
 786 turnover, $J_{\infty\text{H}^+}$, and ATP turnover, $J_{\infty\text{P}}$, proceed in the steady-state at constant $F_{\text{H}^+,\text{out}}$, when $J_{\infty\text{H}^+}$
 787 $= J_{\text{H}^+,\text{out}} = J_{\text{H}^+,\text{in}}$, and at constant $F_{\text{P}\gg}$, when $J_{\infty\text{P}} = J_{\text{P}\gg} = J_{\ll\text{P}}$ (**Fig. 2**).

788

789 **Box 3: Endergonic and exergonic transformations, exergy and dissipation**

790 A chemical reaction, or any transformation, is exergonic if the Gibbs energy change (exergy)
 791 of the reaction is negative at constant temperature and pressure. The sum of Gibbs energy
 792 changes of all internal transformations in a system can only be negative, *i.e.* exergy is

793 irreversibly dissipated. Endergonic reactions are characterized by positive Gibbs energies of
794 reaction and cannot proceed spontaneously in the forward direction as defined. For instance,
795 the endergonic reaction $P \gg$ is coupled to exergonic catabolic reactions, such that the total Gibbs
796 energy change is negative, *i.e.* exergy must be dissipated for the reaction to proceed (**Fig. 2**).

797 In contrast, energy cannot be lost or produced in any internal process, which is the key
798 message of the first law of thermodynamics. Thus mitochondria are the sites of energy
799 transformation but not energy production. Open and closed systems can gain energy and exergy
800 only by external fluxes, *i.e.* uptake from the environment. Exergy is the potential to perform
801 work. In the framework of flux-force relationships (**Box 4**), the *partial* derivative of Gibbs
802 energy per advancement of a transformation is an isomorphic force, F_{tr} (**Table 5**, Note 2). In
803 other words, force is equal to exergy/motive unit (in integral form, this definition takes care of
804 non-isothermal processes). This formal generalization represents an appreciation of the
805 conceptual beauty of Peter Mitchell's innovation of the protonmotive force against the
806 background of the established paradigm of the electromotive force (emf) defined at the limit of
807 zero current (Cohen *et al.* 2008).

808

809 3.3. Forces and fluxes in physics and irreversible thermodynamics

810 According to its definition in physics, a potential difference and as such the
811 *protonmotive force*, Δp_{H^+} , is not a force *per se* (Cohen *et al.* 2008). The fundamental forces of
812 physics are distinguished from *motive forces* of statistical and irreversible thermodynamics.
813 Complementary to the attempt towards unification of fundamental forces defined in physics,
814 the concepts of Nobel laureates Lars Onsager, Erwin Schrödinger, Ilya Prigogine and Peter
815 Mitchell (even if expressed in apparently unrelated terms) unite the diversity of *generalized* or
816 'isomorphic' *flux-force* relationships, the product of which links to the dissipation function and
817 Second Law of thermodynamics (Schrödinger 1944; Prigogine 1967). A *motive force* is the
818 derivative of potentially available or 'free' energy (exergy) per isomorphic *motive* unit (**Box 3**).

819 Perhaps the first account of a *motive force* in energy transformation can be traced back to the
 820 Peripatetic school around 300 BC in the context of moving a lever, up to Newton's motive force
 821 proportional to the alteration of motion (Coopersmith 2010).

822

823 **Table 5. Power, exergy, force, flux, and advancement.**

824

Expression	Symbol	Definition	Unit	Notes
Power, volume-specific	$P_{V,tr}$	$P_{V,tr} = J_{tr} \cdot F_{tr} = \partial_{tr}G \cdot \partial t^{-1}$	$W = J \cdot s^{-1} \cdot m^{-3}$	1
Force, isomorphic	F_{tr}	$F_{tr} = \partial_{tr}G \cdot \partial_{tr}\xi^{-1}$	$J \cdot x^{-1}$	2
Flux, isomorphic	J_{tr}	$J_{tr} = d_{tr}\xi \cdot dt^{-1} \cdot V^{-1}$	$x \cdot s^{-1} \cdot m^{-3}$	3
Advancement, n	$d_{tr}\xi_{H+/n}$	$d_{tr}\xi_{H+/n} = d_{tr}n_{H+} \cdot \nu_{H+}^{-1}$	mol	4n
Advancement, e	$d_{tr}\xi_{H+/e}$	$d_{tr}\xi_{H+/e} = d_{tr}e_{H+} \cdot \nu_{H+}^{-1}$	C	4e
Electric partial force, e	$F_{el/e}$	$F_{el/e} \equiv \Delta\Psi$	V	5e
Electric partial force, n	$F_{el/n}$	$\Delta\Psi \cdot F = 96.5 \cdot \Delta\Psi$	$kJ \cdot mol^{-1}$	5n
Chemical partial force, e	$F_{d,H+/e}$	$\Delta\mu_{H+}/F =$ $-\ln(10) \cdot RT/F \cdot \Delta pH$	V	6e
	at 37 °C	$= -0.06 \cdot \Delta pH$	$J \cdot C^{-1}$	
Chemical partial force, n	$F_{d,H+/n}$	$\Delta\mu_{H+} = -\ln(10) \cdot RT \cdot \Delta pH$	$J \cdot mol^{-1}$	6n
	at 37 °C	$= -5.9 \cdot \Delta pH$	$kJ \cdot mol^{-1}$	

825

826 1 to 4: An isomorphic motive entity or transformant, expressed in units x , is defined for any
 827 transformation, tr . $x = \text{mol}$ or C in proton translocation.

828 2: $\partial_{tr}G$ [J] is the partial Gibbs energy change in the advancement of transformation tr .

829 3: For $x = C$, flow is electric current, I_{el} [$A = C \cdot s^{-1}$], vector flux is electric current density per area, J_{el} ,
 830 and compartmental flux is electric current density per volume, I_{el} [$A \cdot m^{-3}$].

831 4n: For a chemical reaction, the advancement of reaction r is $d_r\xi_B = d_r n_B \cdot \nu_B^{-1}$ [mol]. The stoichiometric
 832 number is $\nu_B = -1$ or $\nu_B = 1$, depending on B being a product or substrate, respectively, in reaction
 833 r involving one mole of B . The conjugated *intensive* molar quantity, $F_{B,r} = \partial_r G / \partial_r \xi_B$ [$J \cdot mol^{-1}$], is the
 834 chemical force of reaction or *reaction-motive* force per stoichiometric amount of B . In reaction
 835 kinetics, $d_r n_B$ is expressed as a volume-specific quantity, which is the partial contribution to the
 836 total concentration change of B , $d_r c_B = d_r n_B / V$ and $d_c c_B = d n_B / V$, respectively. In open systems with
 837 constant volume V , $d_c c_B = d_r c_B + d_e c_B$, where r indicates the *internal* reaction and e indicates the
 838 *external* flux of B into the unit volume of the system. At steady state the concentration does not

839 change, $d_{cB} = 0$, when $d_{r_{cB}}$ is compensated for by the external flux of B, $d_{r_{cB}} = -d_{e_{cB}}$ (Gnaiger
840 1993b). Alternatively, $d_{cB} = 0$ when B is held constant by different coupled reactions in which B
841 acts as a substrate or a product.

842 4e: Scalar potential difference across the mitochondrial membrane. In a scalar electric transformation
843 (flux of charge, *i.e.* volume-specific current, from the matrix space to the intermembrane and
844 extramitochondrial space) the motive force is the difference of charge (**Box 2**). The endergonic
845 direction of translocation is defined in **Fig. 2** as $H^{+}_{in} \rightarrow H^{+}_{out}$.

846 5n: $F = 96.5 \text{ (kJ}\cdot\text{mol}^{-1})/\text{V}$.

847 6: The electric partial force is independent of temperature (Note 5), but the chemical partial force
848 depends on absolute temperature, T [K].

849 6e: RT is the gas constant times absolute temperature. $\ln(10)\cdot RT/F = 59.16$ and 61.54 mV at 298.15
850 and 310.15 K (25 and 37 °C), respectively.

851 6n: $\ln(10)\cdot RT = 5.708$ and 5.938 kJ \cdot mol $^{-1}$ at 298.15 and 310.15 K (25 and 37 °C), respectively.

852

853 **Vectorial and scalar forces, and fluxes:** In chemical reactions and osmotic or diffusion
854 processes occurring in a closed heterogeneous system, such as a chamber containing isolated
855 mitochondria, scalar transformations occur without measured spatial direction but between
856 separate compartments (translocation between the matrix and intermembrane space) or between
857 energetically-separated chemical substances (reactions from substrates to products). Hence, the
858 corresponding fluxes are not vectorial but scalar, and are expressed per volume and not per
859 membrane area (**Box 2**). The corresponding motive forces are also scalar potential *differences*
860 across the membrane (**Table 5**), without taking into account the *gradients* across the 6 nm thick
861 mtIM (Rich 2003).

862 **Coupling:** In energetics (ergodynamics), coupling is defined as an energy transformation
863 fuelled by an exergonic (downhill) input process driving the advancement of an endergonic
864 (uphill) output process. The (negative) output/input power ratio is the efficiency of a coupled
865 energy transformation (**Box 4**). At the limit of maximum efficiency of a completely coupled
866 system, the (negative) input power equals the (positive) output power, such that the total power

867 approaches zero at the maximum efficiency of 1, and the process becomes fully reversible
868 without any dissipation of exergy, *i.e.* without entropy production.

869

870 **Box 4: Coupling, power and efficiency, at constant temperature and pressure**

871 Energetic coupling means that two processes of energy transformation are linked such that the
872 input power, P_{in} , is the driving element of the output power, P_{out} , and the out/input power ratio
873 is the efficiency. In general, power is work per unit time [$J \cdot s^{-1} = W$]. When describing a system
874 with volume V without information on the internal structure, the output is defined as the *external*
875 work (exergy) performed by the *total* system on its environment. Such a system may be open
876 for any type of exchange, or closed and thus allowing only heat and work to be exchanged
877 across the system boundaries. This is the classical black box approach of thermodynamics. In
878 contrast, in a colourful compartmental analysis of *internal* energy transformations (**Fig. 2**), the
879 system is structured and described by definition of ergodynamic compartments (with
880 information on the heterogeneity of the system; **Box 2**) and analysis of separate parts, *i.e.* a
881 sequence of *partial* energy transformations, tr. In general, power per unit volume, P_{tr}/V [$W \cdot L^{-1}$],
882 is the product of a volume-specific flux, J_{tr} , and its conjugated force, F_{tr} , and is closely linked
883 to the dissipation function using the terminology of irreversible thermodynamics (Prigogine
884 1967; Gnaiger 1993a,b). Output power of proton translocation and catabolic input power are
885 (**Fig. 2**),

886 Output:
$$P_{H+,out}/V = J_{H+,out} \cdot F_{H+,out}$$

887 Input:
$$P_k/V = J_{O2,k} \cdot F_{O2,k}$$

888 $F_{O2,k}$ is the exergonic input force with a negative sign, and, $F_{H+,out}$, is the endergonic output
889 force with a positive sign (**Box 3**). Ergodynamic efficiency is the ratio of output/input power,
890 or the flux ratio times force ratio (Gnaiger 1993a,b),

891
$$\varepsilon = \frac{P_{H+,out}}{-P_k} = \frac{J_{H+,out}}{J_{O2,k}} \cdot \frac{F_{H+,out}}{-F_{O2,k}}$$

892 The concept of incomplete coupling relates exclusively to the first term, *i.e.* the flux ratio, or
 893 H^+_{out}/O_2 ratio (**Fig. 1**). Likewise, respirometric definitions of the P_{\gg}/O_2 ratio and biochemical
 894 coupling efficiency (Section 3.2) consider flux ratios. In a completely coupled process, the
 895 power efficiency, ε , depends entirely on the force ratio, ranging from zero efficiency at an
 896 output force of zero, to the limiting output force and maximum efficiency of 1.0, when the total
 897 power of the coupled process, $P_t = P_k + P_{H^+,out}$, equals zero, and any net flows are zero at
 898 ergodynamic equilibrium of a coupled process. Thermodynamic equilibrium is defined as the
 899 state when all potentials (all forces) are dissipated and equilibrate towards their minima of zero.
 900 In a fully or completely coupled process, output and input fluxes are directly proportional in a
 901 fixed ratio technically defined as a stoichiometric relationship (a gear ratio in a mechanical
 902 system). Such maximal stoichiometric output/input flux ratios are considered in OXPHOS
 903 analysis as the upper limits or mechanistic H^+_{out}/O_2 and P_{\gg}/O_2 ratios (**Fig. 1**).

904

905 **Coupled versus bound processes:** Since the chemiosmotic theory describes the
 906 mechanisms of coupling in OXPHOS, it may be interesting to ask if the electrical and chemical
 907 parts of proton translocation are coupled processes. This is not the case according to the
 908 definition of coupling. If the coupling mechanism is disengaged, the output process becomes
 909 independent of the input process, and both proceed in their downhill (exergonic) direction (**Fig.**
 910 **2**). It is not possible to physically uncouple the electrical and chemical processes, which are
 911 only *theoretically* partitioned as electrical and chemical components. The electrical and
 912 chemical partial protonmotive *forces*, $F_{el,out}$ and $F_{H^+,out,d}$, can be measured separately. In
 913 contrast, the corresponding proton *flux*, $J_{H^+,out}$, is non-separable, *i.e.*, cannot be uncoupled. Then
 914 these are not *coupled* processes, but are defined as *bound* processes. The electrical and chemical
 915 parts are tightly bound partial forces, since the flux cannot be partitioned but expressed only in
 916 either an electrical or chemical isomorphic format, $J_{H^+,out/e}$ or $J_{H^+,out/n}$ (**Table 4**).

917

918 4. Normalization: fluxes and flows

919 The challenges of measuring mitochondrial respiratory flux are matched by those of
 920 normalization, whereby O_2 consumption may be considered as the numerator and normalization
 921 as the complementary denominator, which are tightly linked in reporting the measurements in
 922 a format commensurate with the requirements of a database.

923

924 4.1. Flux per chamber volume

925 When the reactor volume does not change during the reaction, which is typical for liquid
 926 phase reactions, the volume-specific *flux of a chemical reaction* r is the time derivative of the
 927 advancement of the reaction per unit volume, $J_{V,B} = d_r \zeta_B / dt \cdot V^{-1}$ [$(\text{mol} \cdot \text{s}^{-1}) \cdot \text{L}^{-1}$]. The *rate of*
 928 *concentration change* is dc_B/dt [$(\text{mol} \cdot \text{L}^{-1}) \cdot \text{s}^{-1}$], where concentration is $c_B = n_B/V$. It is helpful to
 929 make the subtle distinction between [$\text{mol} \cdot \text{s}^{-1} \cdot \text{L}^{-1}$] and [$\text{mol} \cdot \text{L}^{-1} \cdot \text{s}^{-1}$] for the fundamentally
 930 different quantities of volume-specific flux and rate of concentration change, which merge to a
 931 single expression only in closed systems. In open systems, external fluxes (such as O_2 supply)
 932 are distinguished from internal transformations (metabolic flux, O_2 consumption). In a closed
 933 system, external flows of all substances are zero and O_2 consumption (internal flow), I_{O_2}
 934 [$\text{pmol} \cdot \text{s}^{-1}$], causes a decline of the amount of O_2 in the system, n_{O_2} [nmol]. Normalization of
 935 these quantities for the volume of the system, V [$\text{L} = \text{dm}^3$], yields volume-specific O_2 flux, J_{V,O_2}
 936 $= I_{O_2}/V$ [$\text{nmol} \cdot \text{s}^{-1} \cdot \text{L}^{-1}$], and O_2 concentration, $[O_2]$ or $c_{O_2} = n_{O_2}/V$ [$\text{nmol} \cdot \text{mL}^{-1} = \mu\text{mol} \cdot \text{L}^{-1} = \mu\text{M}$].
 937 Instrumental background O_2 flux is due to external flux into a non-ideal closed respirometer,
 938 such that total volume-specific flux has to be corrected for instrumental background O_2 flux,
 939 *i.e.* O_2 diffusion into or out of the instrumental chamber. J_{V,O_2} is relevant mainly for
 940 methodological reasons and should be compared with the accuracy of instrumental resolution
 941 of background-corrected flux, *e.g.* $\pm 1 \text{ nmol} \cdot \text{s}^{-1} \cdot \text{L}^{-1}$ (Gnaiger 2001). ‘Metabolic’ or catabolic
 942 indicates O_2 flux, $J_{O_2,k}$, corrected for instrumental background O_2 flux and chemical background
 943 O_2 flux due to autoxidation of chemical components added to the incubation medium.

944

945 4.2. System-specific and sample-specific normalization

946 Application of common and generally defined units is required for direct transfer of
 947 reported results into a database. The second [s] is the *SI* unit for the base quantity *time*. It is also
 948 the standard time-unit used in solution chemical kinetics. **Table 6** lists some conversion factors
 949 to obtain *SI* units. The term *rate* is not sufficiently defined to be useful for a database (**Fig. 7**).
 950 The inconsistency of the meanings of rate becomes fully apparent when considering Galileo
 951 Galilei's famous principle, that 'bodies of different weight all fall at the same rate (have a
 952 constant acceleration)' (Coopersmith 2010).

953 **Extensive quantities:** An extensive quantity increases proportionally with system size.
 954 The magnitude of an extensive quantity is completely additive for non-interacting subsystems,
 955 such as mass or flow expressed per defined system. The magnitude of these quantities depends
 956 on the extent or size of the system (Cohen *et al.* 2008).

957

958 **Fig. 7. Different meanings of rate**959 **may lead to confusion, if the**960 **normalization is not sufficiently**961 **specified.** Results are frequently962 expressed as mass-specific flux, J_m ,

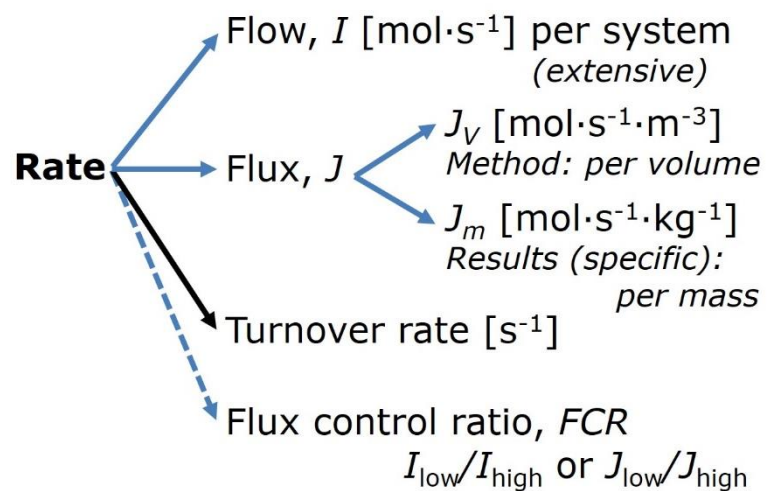
963 per mg protein, dry or wet weight

964 (mass). Cell volume, V_{cell} , or965 mitochondrial volume, V_{mt} , may be

966 used for normalization (volume-

967 specific flux, $J_{V_{\text{cell}}}$ or $J_{V_{\text{mt}}}$), which then must be clearly distinguished from flux, J_v , expressed for968 methodological reasons per volume of the measurement system, or flow per cell, I_x .

969

970 **Size-specific quantities:** 'The adjective *specific* before the name of an extensive quantity971 is often used to mean *divided by mass*' (Cohen *et al.* 2008). Mass-specific flux is flow divided

969

970 **Size-specific quantities:** 'The adjective *specific* before the name of an extensive quantity971 is often used to mean *divided by mass*' (Cohen *et al.* 2008). Mass-specific flux is flow divided

972 by mass of the system. A mass-specific quantity is independent of the extent of non-interacting
 973 homogenous subsystems. Tissue-specific quantities are of fundamental interest in comparative
 974 mitochondrial physiology, where *specific* refers to the *type* rather than *mass* of the tissue. The
 975 term *specific*, therefore, must be further clarified, such that tissue mass-specific, *e.g.*, muscle
 976 mass-specific quantities are defined.

977 **Molar quantities:** ‘The adjective *molar* before the name of an extensive quantity
 978 generally means *divided by amount of substance*’ (Cohen *et al.* 2008). The notion that all molar
 979 quantities then become *intensive* causes ambiguity in the meaning of *molar Gibbs energy*. It is
 980 important to emphasize the fundamental difference between normalization for amount of
 981 substance *in a system* or for amount of motive substance *in a transformation*. When the Gibbs
 982 energy of a system, G [J], is divided by the amount of substance B in the system, n_B [mol], a
 983 *size-specific* molar quantity is obtained, $G_B = G/n_B$ [J·mol⁻¹], which is not any force at all. In
 984 contrast, when the partial Gibbs energy change, $\partial_r G$ [J], is divided by the motive amount of
 985 substance B in reaction r (advancement of reaction), $\partial_r \xi_B$ [mol], the resulting intensive molar
 986 quantity, $F_{B,r} = \partial G / \partial_r \xi_B$ [J·mol⁻¹], is the chemical motive force of reaction r involving 1 mol B
 987 (**Table 5**, Note 4).

988 **Flow per system, I :** In analogy to electrical terms, flow as an extensive quantity (I ; per
 989 system) is distinguished from flux as a size-specific quantity (J ; per system size) (**Fig. 7**).
 990 Electric current is flow, I_{el} [A = C·s⁻¹] per system (extensive quantity). When dividing this
 991 extensive quantity by system size (membrane area), a size-specific quantity is obtained, which
 992 is electric flux (electric current density), J_{el} [A·m⁻² = C·s⁻¹·m⁻²].

993 **Size-specific flux, J :** Metabolic O₂ flow per tissue increases as tissue mass is increased.
 994 Tissue mass-specific O₂ flux should be independent of the size of the tissue sample studied in
 995 the instrument chamber, but volume-specific O₂ flux (per volume of the instrument chamber,
 996 V) should increase in direct proportion to the amount of sample in the chamber. Accurate
 997 definition of the experimental system is decisive: whether the experimental chamber is the

998 closed, open, isothermal or non-isothermal *system* with defined volume as part of the
999 measurement apparatus, in contrast to the experimental *sample* in the chamber (**Table 6**).
1000 Volume-specific O₂ flux depends on mass-concentration of the sample in the chamber, but
1001 should be independent of the chamber volume. There are practical limitations to increasing the
1002 mass-concentration of the sample in the chamber, when one is concerned about crowding
1003 effects and instrumental time resolution.

1004 **Sample concentration C_{mX} :** Normalization for sample concentration is required for
1005 reporting respiratory data. Consider a tissue or cells as the sample, X , and the sample mass, m_X
1006 [mg] from which a mitochondrial preparation is obtained. The sample mass, m_X , is frequently
1007 measured as wet or dry weight, W_w or W_d [mg], or as amount of tissue or cell protein, m_{Protein} .
1008 In the case of permeabilized tissues, cells, and homogenates, the sample concentration, $C_{mX} =$
1009 m_X/V [$\text{mg}\cdot\text{mL}^{-1} = \text{g}\cdot\text{L}^{-1}$], is simply the mass of the subsample of tissue that is transferred into
1010 the instrument chamber. Part of the mitochondria from the tissue is lost during preparation of
1011 isolated mitochondria, and only a fraction of mitochondria is obtained, expressed as the
1012 mitochondrial yield (**Fig. 8**). At a high mitochondrial yield the sample of isolated mitochondria
1013 is more representative of the total mitochondrial population than in preparations characterized
1014 by low mitochondrial yield. Determination of the mitochondrial yield is based on measurement
1015 of the concentration of a mitochondrial marker in the tissue homogenate, $C_{\text{mte,thom}}$, which
1016 simultaneously provides information on the specific mitochondrial density in the sample (**Fig.**
1017 **8**).

1018 Tissues can contain multiple cell populations which may have distinct mitochondrial
1019 subtypes. Mitochondria are also in a constant state of flux due to highly dynamic fission and
1020 fusion cycles, and can exist in multiple stages and sizes which may be altered by a range of
1021 factors. The isolation of mitochondria (often achieved through differential centrifugation) can
1022 therefore yield a subsample of the mitochondrial types present in a tissue, dependent on
1023 isolation protocols utilized (*e.g.* centrifugation speed). This possible artefact should be taken

1024 into account when planning experiments using isolated mitochondria. The tendency for
 1025 mitochondria of specific sizes to be enriched at different centrifugation speeds also has the
 1026 potential to allow the isolation of specific mitochondrial subpopulations and therefore the
 1027 analysis of mitochondria from multiple cell lineages within a single tissue.

1028

1029 **Table 6. Sample concentrations and normalization of flux with SI base units.**

Expression	Symbol	Definition	SI Unit	Notes
Sample				
Identity of sample	X	Cells, animals, patients		
Number of sample entities X	N_X	Number of cells, <i>etc.</i>	x	
Mass of sample X	m_X		kg	1
Mass of entity X	M_X	$M_X = m_X \cdot N_X^{-1}$	$\text{kg} \cdot \text{x}^{-1}$	1
Mitochondria				
Mitochondria	mt	$X = \text{mt}$		
Amount of mt-elements	mte	Quantity of mt-marker	x_{mte}	
Concentrations				
Sample number concentration	C_{NX}	$C_{NX} = N_X \cdot V^{-1}$	$\text{x} \cdot \text{m}^{-3}$	2
Sample mass concentration	C_{mX}	$C_{mX} = m_X \cdot V^{-1}$	$\text{kg} \cdot \text{m}^{-3}$	
Mitochondrial concentration	C_{mte}	$C_{\text{mte}} = \text{mte} \cdot V^{-1}$	$x_{\text{mte}} \cdot \text{m}^{-3}$	3
Specific mitochondrial density	D_{mte}	$D_{\text{mte}} = \text{mte} \cdot m_X^{-1}$	$x_{\text{mte}} \cdot \text{kg}^{-1}$	4
Mitochondrial content, mte per entity X	mte_X	$\text{mte}_X = \text{mte} \cdot N_X^{-1}$	$x_{\text{mte}} \cdot \text{x}^{-1}$	5
O₂ flow and flux				
Flow	I_{O_2}	Internal flow	$\text{mol} \cdot \text{s}^{-1}$	6
Volume-specific flux	J_{V,O_2}	$J_{V,\text{O}_2} = I_{\text{O}_2} \cdot V^{-1}$	$\text{mol} \cdot \text{s}^{-1} \cdot \text{m}^{-3}$	7
Flow per sample entity X	I_{X,O_2}	$I_{X,\text{O}_2} = J_{V,\text{O}_2} \cdot C_{NX}^{-1}$	$\text{mol} \cdot \text{s}^{-1} \cdot \text{x}^{-1}$	8
Mass-specific flux	J_{mX,O_2}	$J_{mX,\text{O}_2} = J_{V,\text{O}_2} \cdot C_{mX}^{-1}$	$\text{mol} \cdot \text{s}^{-1} \cdot \text{kg}^{-1}$	9
Mitochondria-specific flux	$J_{\text{mte},\text{O}_2}$	$J_{\text{mte},\text{O}_2} = J_{V,\text{O}_2} \cdot C_{\text{mte}}^{-1}$	$\text{mol} \cdot \text{s}^{-1} \cdot x_{\text{mte}}^{-1}$	10

1031

1032 1 The SI prefix k is used for the SI base unit of mass (kg = 1,000 g). In praxis, various SI prefixes are
 1033 used for convenience, to make numbers easily readable, e.g. 1 mg tissue, cell or mitochondrial mass
 1034 instead of 0.000001 kg.

1035 2 In case $X = \text{cells}$, the sample number concentration is $C_{N_{\text{cell}}} = N_{\text{cell}} \cdot V^{-1}$, and volume may be expressed
 1036 in [$\text{dm}^3 = \text{L}$] or [$\text{cm}^3 = \text{mL}$]. See **Table 7** for different sample types.

1037 3 mt-concentration is an experimental variable, dependent on sample concentration: (1) $C_{\text{mte}} = \text{mte} \cdot V^{-1}$;
 1038 (2) $C_{\text{mte}} = \text{mte}_X \cdot C_{NX}$; (3) $C_{\text{mte}} = C_{mX} \cdot D_{\text{mte}}$.

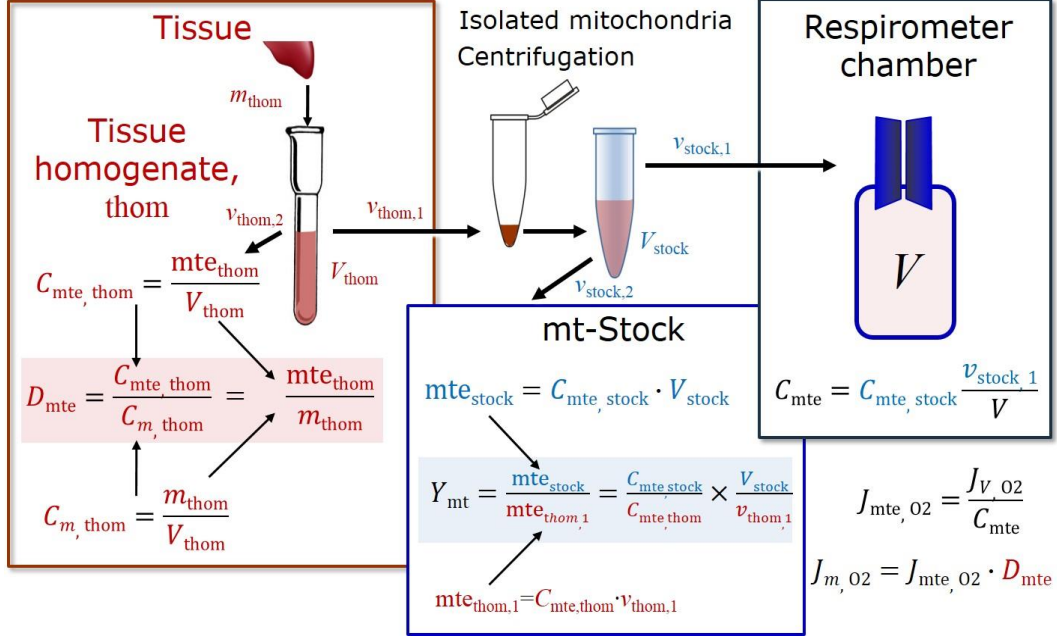
- 1039 4 If the amount of mitochondria, m_{te} , is expressed as mitochondrial mass, then D_{mte} is the mass
 1040 fraction of mitochondria in the sample. If m_{te} is expressed as mitochondrial volume, V_{mt} , and the
 1041 mass of sample, m_X , is replaced by volume of sample, V_X , then D_{mte} is the volume fraction of
 1042 mitochondria in the sample.
- 1043 5 $m_{teX} = m_{te} \cdot N_X^{-1} = C_{mte} \cdot C_{NX}^{-1}$.
- 1044 6 Entity O_2 can be replaced by other chemical entities B to study different reactions.
- 1045 7 I_{O_2} and V are defined per instrument chamber as a system of constant volume (and constant
 1046 temperature), which may be closed or open. I_{O_2} is abbreviated for $I_{O_2,r}$, *i.e.* the metabolic or internal
 1047 O_2 flow of the chemical reaction r in which O_2 is consumed, hence the negative stoichiometric
 1048 number, $\nu_{O_2} = -1$. $I_{O_2,r} = d_r n_{O_2} / dt \cdot \nu_{O_2}^{-1}$. If r includes all chemical reactions in which O_2 participates,
 1049 then $d_r n_{O_2} = dn_{O_2} - d_e n_{O_2}$, where dn_{O_2} is the change in the amount of O_2 in the instrument chamber
 1050 and $d_e n_{O_2}$ is the amount of O_2 added externally to the system. At steady state, by definition $dn_{O_2} = 0$,
 1051 hence $d_r n_{O_2} = -d_e n_{O_2}$.
- 1052 8 J_{V,O_2} is an experimental variable, expressed per volume of the instrument chamber.
- 1053 9 I_{X,O_2} is a physiological variable, depending on the size of entity X .
- 1054 10 There are many ways to normalize for a mitochondrial marker, that are used in different experimental
 1055 approaches: (1) $J_{mte,O_2} = J_{V,O_2} \cdot C_{mte}^{-1}$; (2) $J_{mte,O_2} = J_{V,O_2} \cdot C_{mX}^{-1} \cdot D_{mte}^{-1} = J_{mX,O_2} \cdot D_{mte}^{-1}$; (3) $J_{mte,O_2} =$
 1056 $J_{V,O_2} \cdot C_{NX}^{-1} \cdot m_{teX}^{-1} = I_{X,O_2} \cdot m_{teX}^{-1}$; (4) $J_{mte,O_2} = I_{O_2} \cdot m_{te}^{-1}$.

1057

1058 **Mass-specific flux, J_{mX,O_2} :** Mass-specific flux is obtained by expressing respiration per
 1059 mass of sample, m_X [mg]. X is the type of sample, *e.g.*, tissue homogenate, permeabilized fibres
 1060 or cells. Volume-specific flux is divided by mass concentration of X , $J_{mX,O_2} = J_{V,O_2} / C_{mX}$; or flow
 1061 per cell is divided by mass per cell, $J_{mcell,O_2} = I_{cell,O_2} / M_{cell}$. If mass-specific O_2 flux is constant
 1062 and independent of sample size (expressed as mass), then there is no interaction between the
 1063 subsystems. A 1.5 mg and a 3.0 mg muscle sample respire at identical mass-specific flux.
 1064 Mass-specific O_2 flux, however, may change with the mass of a tissue sample, cells or isolated
 1065 mitochondria in the measuring chamber, in which case the nature of the interaction becomes an
 1066 issue. Optimization of cell density and arrangement is generally important and particularly in

1067 experiments carried out in wells, considering the confluency of the cell monolayer or clumps
 1068 of cells (Salabei *et al.* 2014).

1069



1070

Symbol	Definition [Units]
C_{mte}	Mitochondrial concentration in chamber [$x_{mte} \cdot L^{-1}$]
C_m	Sample mass concentration in chamber [$g \cdot L^{-1}$]
D_{mte}	Specific mte-density per tissue mass [$x_{mte} \cdot g^{-1}$]
J_{m,O_2}	Mass-specific O_2 flux [$nmol \cdot s^{-1} \cdot g^{-1}$]
J_{mte,O_2}	Mitochondria-specific O_2 flux [$nmol \cdot s^{-1} \cdot x_{mte}^{-1}$]
mte	Amount of mitochondrial elements [x_{mte}]
m_{thom}	Mass of tissue in the homogenate [g]
Y_{mt}	Yield of isolated mitochondria

Respirometer chamber

Homogenate

$v_{thom,1}$

V

$$C_m = C_{m,thom} \frac{v_{thom,1}}{V}$$

$$C_{mte} = C_m \cdot D_{mte}$$

$$J_{m,O_2} = \frac{J_{V,O_2}}{C_m}$$

$$J_{mte,O_2} = \frac{J_{m,O_2}}{D_{mte}}$$

1071

1072 **Fig. 8. Normalization of volume-specific flux of isolated mitochondria and tissue**

1073 **homogenate. A:** Mitochondrial yield, Y_{mt} , in preparation of isolated mitochondria. $v_{thom,1}$

1074 and $v_{stock,1}$ are the volumes transferred from the total volume, V_{thom} and V_{stock} , respectively.

1075 $mte_{thom,1}$ is the amount of mitochondrial elements in volume $v_{thom,1}$ used for isolation. **B:**

1076 In respirometry with homogenate, $v_{thom,1}$ is transferred directly into the respirometer

1077 chamber. See **Table 6** for further explanation of symbols.

1078

1079

1080

Table 7. Some useful abbreviations of various sample types, X.

Identity of sample	X
Mitochondrial preparation	mtprep
Isolated mitochondria	imt
Tissue homogenate	thom
Permeabilized tissue	pti
Permeabilized fibre	pfi
Permeabilized cell	pce
Cell	ce
Organism	org

1081

1082

1083

1084

Number concentration, C_{NX} : The experimental *number concentration* of sample in the case of cells or animals, *e.g.*, nematodes is $C_{NX} = N_X/V$ [$x \cdot mL^{-1}$], where N_X is the number of cells or organisms in the chamber (**Table 6**).

1085

1086

1087

1088

1089

1090

1091

1092

1093

Flow per sample entity, I_{X,O_2} : A special case of normalization is encountered in respiratory studies with permeabilized (or intact) cells. If respiration is expressed per cell, the O_2 flow per measurement system is replaced by the O_2 flow per cell, I_{cell,O_2} (**Table 6**). O_2 flow can be calculated from volume-specific O_2 flux, J_{V,O_2} [$nmol \cdot s^{-1} \cdot L^{-1}$] (per V of the measurement chamber [L]), divided by the number concentration of cells, $C_{N_{ce}} = N_{ce}/V$ [$cell \cdot L^{-1}$], where N_{ce} is the number of cells in the chamber. Cellular O_2 flow can be compared between cells of identical size. To take into account changes and differences in cell size, further normalization is required to obtain cell size-specific or mitochondrial marker-specific O_2 flux (Renner *et al.* 2003).

1094

1095

1096

The complexity changes when the sample is a whole organism studied as an experimental model. The well-established scaling law in respiratory physiology reveals a strong interaction of O_2 consumption and individual body mass of an organism, since *basal* metabolic rate (flow)

1097 does not increase linearly with body mass, whereas *maximum* mass-specific O₂ flux, $\dot{V}_{O_{2max}}$ or
1098 $\dot{V}_{O_{2peak}}$, is approximately constant across a large range of individual body mass (Weibel and
1099 Hoppeler 2005), with individuals, breeds, and certain species deviating substantially from this
1100 general relationship. $\dot{V}_{O_{2peak}}$ of human endurance athletes is 60 to 80 mL O₂·min⁻¹·kg⁻¹ body
1101 mass, converted to $J_{m,O_{2peak}}$ of 45 to 60 nmol·s⁻¹·g⁻¹ (Gnaiger 2014; **Table 8**).

1102

1103 *4.3. Normalization for mitochondrial content*

1104 Normalization is a problematic subject and it is essential to consider the question of the
1105 study. If the study aims to compare tissue performance, such as the effects of a certain treatment
1106 on a specific tissue, then normalization can be successful, using tissue mass or protein content,
1107 for example. If the aim, however, is to find differences of mitochondrial function independent
1108 of mitochondrial density (**Table 6**), then normalization to a mitochondrial marker is imperative
1109 (**Fig. 9**). However, one cannot assume that quantitative changes in various markers such as
1110 mitochondrial proteins necessarily occur in parallel with one another. It is important to first
1111 establish that the marker chosen is not selectively altered by the performed treatment. In
1112 conclusion, the normalization must reflect the question under investigation to reach a satisfying
1113 answer. On the other hand, the goal of comparing results across projects and institutions
1114 requires some standardization on normalization for entry into a databank.

1115 **Mitochondrial concentration, C_{mte} , and mitochondrial markers:** It is important that
1116 mitochondrial concentration in the tissue and the measurement chamber be quantified, as a
1117 physiological output and result of mitochondrial biogenesis and degradation, and as a quantity
1118 for normalization in functional analyses. Mitochondrial organelles comprise a cellular
1119 reticulum that is in a continual flux of fusion and fission. Hence the definition of an "amount"
1120 of mitochondria is often misconceived: mitochondria cannot be counted as a number of
1121 occurring elements. Therefore, quantification of the "amount" of mitochondria depends on
1122 measurement of chosen mitochondrial markers. 'Mitochondria are the structural and functional

1123 elemental units of cell respiration' (Gnaiger 2014). The quantity of a mitochondrial marker can
 1124 be considered as the measurement of the amount of *elemental mitochondrial units* or
 1125 *mitochondrial elements*, mte. However, since mitochondrial quality changes under certain
 1126 stimuli, particularly in mitochondrial dysfunction and after exercise training (Pesta *et al.* 2011;
 1127 Campos *et al.* 2017), some markers can vary while other markers are unchanged. (1)
 1128 Mitochondrial volume and membrane area are structural markers, whereas mitochondrial
 1129 protein mass is frequently used as a marker for isolated mitochondria. (2) Molecular and
 1130 enzymatic mitochondrial markers (amounts or activities) can be selected as matrix markers,
 1131 *e.g.*, citrate synthase activity, mtDNA; mtIM-markers, *e.g.*, cytochrome *c* oxidase activity, *aa₃*
 1132 content, cardiolipin, or mtOM-markers, *e.g.*, TOM20. (3) Extending the measurement of
 1133 mitochondrial marker enzyme activity to mitochondrial pathway capacity, measured as ET- or
 1134 OXPHOS-capacity, can be considered as an integrative functional mitochondrial marker.

1135 Depending on the type of mitochondrial marker, the mitochondrial elements, mte, are
 1136 expressed in marker-specific units. Although concentration and density are used synonymously
 1137 in physical chemistry, it is recommended to distinguish *experimental mitochondrial*
 1138 *concentration*, $C_{\text{mte}} = \text{mte}/V$ and *physiological mitochondrial density*, $D_{\text{mte}} = \text{mte}/m_X$. Then
 1139 mitochondrial density is the amount of mitochondrial elements per mass of tissue (Fig. 9). The
 1140 former is mitochondrial density multiplied by sample mass concentration, $C_{\text{mte}} = D_{\text{mte}} \cdot C_{m_X}$, or
 1141 mitochondrial content multiplied by sample number concentration, $C_{\text{mte}} = \text{mte}_X \cdot C_{N_X}$ (Table 6).

1142 **Mitochondria-specific flux, $J_{\text{mte},\text{O}_2}$:** Volume-specific metabolic O₂ flux depends on: (1)
 1143 the sample concentration in the volume of the instrument chamber, C_{m_X} , or C_{N_X} ; (2) the
 1144 mitochondrial density in the sample, $D_{\text{mte}} = \text{mte}/m_X$ or $\text{mte}_X = \text{mte}/N_X$; and (3) the specific
 1145 mitochondrial activity or performance per elemental mitochondrial unit, $J_{\text{mte},\text{O}_2} = J_{V,\text{O}_2}/C_{\text{mte}}$
 1146 (Table 6). Obviously, the numerical results for $J_{\text{mte},\text{O}_2}$ vary according to the type of
 1147 mitochondrial marker chosen for measurement of mte and $C_{\text{mte}} = \text{mte}/V$.

Flow, Performance	=	Element function	x	Element density	x	Size of entity
$\frac{\text{mol}\cdot\text{s}^{-1}}{X}$	=	$\frac{\text{mol}\cdot\text{s}^{-1}}{X_{\text{mte}}}$	·	$\frac{X_{\text{mte}}}{\text{kg}}$	·	$\frac{\text{kg}}{X}$

A	Flow	=	mt-specific flux	x	mt-structure, functional elements
	I_{X,O_2}	=	J_{mte,O_2}	·	mte_X
					$\left(\frac{\text{mte}_X}{M_X} \cdot M_X \right)$

I_{X,O_2}	=	J_{mte,O_2}	·	D_{mte}	·	M_X
$\frac{I_{X,O_2}}{M_X}$	=	$\frac{I_{X,O_2}}{\text{mte}_X}$	·	$\frac{\text{mte}_X}{M_X}$		

B	I_{X,O_2}	=	J_{mX,O_2}	·	M_X
	Flow	=	Entity mass-specific flux	x	Mass of entity

1148
 1149 **Fig. 9. Structure-function analysis of performance of an**
 1150 **organism, organ or tissue, or a cell (sample entity X). O₂**
 1151 **flow, I_{X,O_2} , is the product of performance per functional**
 1152 **element (element function, mitochondria-specific flux),**
 1153 **element density (mitochondrial density, D_{mte}), and size of**
 1154 **entity X (mass M_X). (A) Structured analysis: performance is the**
 1155 **product of mitochondrial function (mt-specific flux) and structure**
 1156 **(functional elements; D_{mte} times mass of X). (B) Unstructured**
 1157 **analysis: performance is the product of entity mass-specific flux,**
 1158 **$J_{mX,O_2} = I_{X,O_2}/M_X = I_{O_2}/m_X$ [mol·s⁻¹·kg⁻¹] and size of entity,**
 1159 **expressed as mass of X; $M_X = m_X \cdot N_X^{-1}$ [kg·x⁻¹]. See Table 6 for**
 1160 **further explanation of quantities and units. Modified from Gnaiger**
 1161 **(2014).**

1163 4.4. Evaluation of mitochondrial markers

1164 Different methods are implicated in quantification of mitochondrial markers and have
 1165 different strengths. Some problems are common for all mitochondrial markers, mte: (I)
 1166 Accuracy of measurement is crucial, since even a highly accurate and reproducible

1167 measurement of O₂ flux results in an inaccurate and noisy expression normalized for a biased
1168 and noisy measurement of a mitochondrial marker. This problem is acute in mitochondrial
1169 respiration because the denominators used (the mitochondrial markers) are often very small
1170 moieties whose accurate and precise determination is difficult. This problem can be avoided
1171 when O₂ fluxes measured in substrate-uncoupler-inhibitor titration protocols are normalized for
1172 flux in a defined respiratory reference state, which is used as an *internal* marker and yields flux
1173 control ratios, *FCRs* (Fig. 7). *FCRs* are independent of any *externally* measured markers and,
1174 therefore, are statistically very robust, considering the limitations of ratios in general (Jasienski
1175 and Bazzaz 1999). *FCRs* indicate qualitative changes of mitochondrial respiratory control, with
1176 highest quantitative resolution, separating the effect of mitochondrial density or concentration
1177 on J_{mX,O_2} and I_{X,O_2} from that of function per elemental mitochondrial marker, J_{mte,O_2} (Pesta *et*
1178 *al.* 2011; Gnaiger 2014). (2) If mitochondrial quality does not change and only the amount of
1179 mitochondria, defined by the chosen mitochondrial marker, varies as a determinant of mass-
1180 specific flux, any marker is equally qualified in principle; then in practice selection of the
1181 optimum marker depends only on the accuracy and precision of measurement of the
1182 mitochondrial marker. (3) If mitochondrial flux control ratios change, then there may not be
1183 any best mitochondrial marker. In general, measurement of multiple mitochondrial markers
1184 enables a comparison and evaluation of normalization for a variety of mitochondrial markers.
1185 Evaluation of mitochondrial markers in healthy controls is insufficient for providing guidelines
1186 for application in the diagnosis of pathological states and specific treatments.

1187 In line with the concept of the respiratory control ratio (Chance and Williams 1955a), the
1188 most readily used normalization is that of flux control ratios and flux control factors (Gnaiger
1189 2014). Selection of the state of maximum flux in a protocol as the reference state has the
1190 advantages of (1) internal normalization, (2) statistical linearization of the response in the range
1191 of 0 to 1, and (3) consideration of maximum flux for integrating a very large number of
1192 elemental steps in the OXPHOS- or ET-pathways. This reduces the risk of selecting a functional

1193 marker that is specifically altered by the treatment or pathodology, yet increases the chance that
1194 the highly integrative pathway is disproportionately affected, *e.g.* the OXPPOS- rather than
1195 ET-pathway in case of an enzymatic defect in the phosphorylation-pathway. In this case,
1196 additional information can be obtained by reporting flux control ratios based on a reference
1197 state which indicates stable tissue-mass specific flux. Stereological determination of
1198 mitochondrial content via two-dimensional transmission electron microscopy can have
1199 limitations due to the dynamics of mitochondrial size (Meinild Lundby *et al.* 2017). Accurate
1200 determination of three-dimensional volume by two-dimensional microscopy can be both time
1201 consuming and statistically challenging (Larsen *et al.* 2012). Using mitochondrial marker
1202 enzymes (citrate synthase activity, Complex I–IV amount or activity) for normalization of flux
1203 is limited in part by the same factors that apply to the use of flux control ratios. Strong
1204 correlations between various mitochondrial markers and citrate synthase activity (Reichmann
1205 *et al.* 1985; Boushel *et al.* 2007; Mogensen *et al.* 2007) are expected in a specific tissue of
1206 healthy subjects and in disease states not specifically targeting citrate synthase. Citrate synthase
1207 activity is acutely modifiable by exercise (Tonkonogi *et al.* 1997; Leek *et al.* 2001). Evaluation
1208 of mitochondrial markers related to a selected age and sex cohort cannot be extrapolated to
1209 provide recommendations for normalization in respirometric diagnosis of disease, in different
1210 states of development and ageing, different cell types, tissues, and species. mtDNA normalised
1211 to nDNA via qPCR is correlated to functional mitochondrial markers including OXPPOS- and
1212 ET-capacity in some cases (Puntschart *et al.* 1995; Wang *et al.* 1999; Menshikova *et al.* 2006;
1213 Boushel *et al.* 2007), but lack of such correlations have been reported (Menshikova *et al.* 2005;
1214 Schultz and Wiesner 2000; Pesta *et al.* 2011). Several studies indicate a strong correlation
1215 between cardiolipin content and increase in mitochondrial functionality with exercise
1216 (Menshikova *et al.* 2005; Menshikova *et al.* 2007; Larsen *et al.* 2012; Faber *et al.* 2014), but its
1217 use as a general mitochondrial biomarker in disease remains questionable.
1218

1219 4.5. Conversion: units and normalization

1220 Many different units have been used to report the rate of oxygen consumption, OCR
1221 (**Table 8**). *SI* base units provide the common reference for introducing the theoretical principles
1222 (**Fig. 7**), and are used with appropriately chosen *SI* prefixes to express numerical data in the
1223 most practical format, with an effort towards unification within specific areas of application
1224 (**Table 9**). For studies of cells, we recommend that respiration be expressed, as far as possible,
1225 as (1) O₂ flux normalized for a mitochondrial marker, for separation of the effects of
1226 mitochondrial quality and content on cell respiration (this includes *FCRs* as a normalization for
1227 a functional mitochondrial marker); (2) O₂ flux in units of cell volume or mass, for comparison
1228 of respiration of cells with different cell size (Renner *et al.* 2003) and with studies on tissue
1229 preparations, and (3) O₂ flow in units of attomole (10⁻¹⁸ mol) of O₂ consumed by each cell in a
1230 second [amol·s⁻¹·cell⁻¹], numerically equivalent to [pmol·s⁻¹·10⁻⁶ cells]. This convention allows
1231 information to be easily used when designing experiments in which oxygen consumption must
1232 be considered. For example, to estimate the volume-specific O₂ flux in an instrument chamber
1233 that would be expected at a particular cell number concentration, one simply needs to multiply
1234 the flow per cell by the number of cells per volume of interest. This provides the amount of O₂
1235 [mol] consumed per time [s⁻¹] per unit volume [L⁻¹]. At an O₂ flow of 100 amol·s⁻¹·cell⁻¹ and a
1236 cell density of 10⁹ cells·L⁻¹ (10⁶ cells·mL⁻¹), the volume-specific O₂ flux is 100 nmol·s⁻¹·L⁻¹ (100
1237 pmol·s⁻¹·mL⁻¹).

1238 Although volume is expressed as m³ using the *SI* base unit, the litre [dm³] is the basic unit
1239 of volume for concentration and is used for most solution chemical kinetics. If one multiplies
1240 $I_{\text{cell},\text{O}_2}$ by C_{Ncell} , then the result will not only be the amount of O₂ [mol] consumed per time [s⁻¹]
1241 in one litre [L⁻¹], but also the change in the concentration of oxygen per second (for any volume
1242 of an ideally closed system). This is ideal for kinetic modeling as it blends with chemical rate
1243 equations where concentrations are typically expressed in mol·L⁻¹ (Wagner *et al.* 2011). In
1244 studies of multinuclear cells, such as differentiated skeletal muscle cells, it is easy to determine

1245 the number of nuclei but not the total number of cells. A generalized concept, therefore, is
 1246 obtained by substituting cells by nuclei as the sample entity. This does not hold, however, for
 1247 enucleated platelets.

1248

1249 **Table 8. Conversion of various units used in respirometry and**
 1250 **ergometry.** e is the number of electrons or reducing equivalents. z_B is the
 1251 charge number of entity B.

1252

1 Unit	x	Multiplication factor	SI-Unit	Note
ng.atom O \cdot s $^{-1}$	(2 e)	0.5	nmol O $_2$ \cdot s $^{-1}$	
ng.atom O \cdot min $^{-1}$	(2 e)	8.33	pmol O $_2$ \cdot s $^{-1}$	
natom O \cdot min $^{-1}$	(2 e)	8.33	pmol O $_2$ \cdot s $^{-1}$	
nmol O $_2$ \cdot min $^{-1}$	(4 e)	16.67	pmol O $_2$ \cdot s $^{-1}$	
nmol O $_2$ \cdot h $^{-1}$	(4 e)	0.2778	pmol O $_2$ \cdot s $^{-1}$	
mL O $_2$ \cdot min $^{-1}$ at STPD a		0.744	μ mol O $_2$ \cdot s $^{-1}$	1
W = J/s at -470 kJ/mol O $_2$		-2.128	μ mol O $_2$ \cdot s $^{-1}$	
mA = mC \cdot s $^{-1}$	($z_{H^+} = 1$)	10.36	nmol H $^+$ \cdot s $^{-1}$	2
mA = mC \cdot s $^{-1}$	($z_{O_2} = 4$)	2.59	nmol O $_2$ \cdot s $^{-1}$	2
nmol H $^+$ \cdot s $^{-1}$	($z_{H^+} = 1$)	0.09649	mA	3
nmol O $_2$ \cdot s $^{-1}$	($z_{O_2} = 4$)	0.38594	mA	3

1253

1254 1 At standard temperature and pressure dry (STPD: 0 $^{\circ}$ C = 273.15 K and 1 atm =
 1255 101.325 kPa = 760 mmHg), the molar volume of an ideal gas, V_m , and V_{m,O_2} is
 1256 22.414 and 22.392 L \cdot mol $^{-1}$ respectively. Rounded to three decimal places, both
 1257 values yield the conversion factor of 0.744. For comparison at NTPD (20 $^{\circ}$ C),
 1258 V_{m,O_2} is 24.038 L \cdot mol $^{-1}$. Note that the SI standard pressure is 100 kPa.

1259 2 The multiplication factor is $10^6/(z_B \cdot F)$.

1260 3 The multiplication factor is $z_B \cdot F/10^6$.

1261

1262 4.5. Conversion: oxygen, proton and ATP flux

1263 $J_{O_2,k}$ is coupled in mitochondrial steady states to proton cycling, $J_{\infty H^+} = J_{H^+,out} = J_{H^+,in}$
 1264 (**Fig. 2**). $J_{H^+,out/n}$ and $J_{H^+,in/n}$ [$\text{nmol}\cdot\text{s}^{-1}\cdot\text{L}^{-1}$] are converted into electrical units, $J_{H^+,out/e}$ [$\text{mC}\cdot\text{s}^{-1}\cdot\text{L}^{-1}$
 1265 $= \text{mA}\cdot\text{L}^{-1}$] = $J_{H^+,out/n}$ [$\text{nmol}\cdot\text{s}^{-1}\cdot\text{L}^{-1}$] $\cdot F$ [$\text{C}\cdot\text{mol}^{-1}$] $\cdot 10^{-6}$ (**Table 4**). At a $J_{H^+,out}/J_{O_2,k}$ ratio or H^+_{out}/O_2
 1266 of 20 ($H^+_{out}/O = 10$), a volume-specific O_2 flux of $100 \text{ nmol}\cdot\text{s}^{-1}\cdot\text{L}^{-1}$ would correspond to a proton
 1267 flux of $2,000 \text{ nmol H}^+_{out}\cdot\text{s}^{-1}\cdot\text{L}^{-1}$ or volume-specific current of $193 \text{ mA}\cdot\text{L}^{-1}$.

$$1268 \quad J_{V,H^+,out/e} [\text{mA}\cdot\text{L}^{-1}] = J_{V,H^+,out/n} \cdot F \cdot 10^{-6} [\text{nmol}\cdot\text{s}^{-1}\cdot\text{L}^{-1} \cdot \text{mC}\cdot\text{nmol}^{-1}] \quad (\text{Eq. 3.1})$$

$$1269 \quad J_{V,H^+,out/e} [\text{mA}\cdot\text{L}^{-1}] = J_{V,O_2} \cdot (H^+_{out}/O_2) \cdot F \cdot 10^{-6} [\text{mC}\cdot\text{s}^{-1}\cdot\text{L}^{-1} = \text{mA}\cdot\text{L}^{-1}] \quad (\text{Eq. 3.2})$$

1270

1271 **Table 9. Conversion of units with preservation of numerical values.**

Name	Frequently used unit	Equivalent unit	Note
Volume-specific flux, J_{V,O_2}	$\text{pmol}\cdot\text{s}^{-1}\cdot\text{mL}^{-1}$	$\text{nmol}\cdot\text{s}^{-1}\cdot\text{L}^{-1}$	1
	$\text{mmol}\cdot\text{s}^{-1}\cdot\text{L}^{-1}$	$\text{mol}\cdot\text{s}^{-1}\cdot\text{m}^{-3}$	
Cell-specific flow, I_{O_2}	$\text{pmol}\cdot\text{s}^{-1}\cdot 10^{-6} \text{ cells}$	$\text{amol}\cdot\text{s}^{-1}\cdot\text{cell}^{-1}$	2
	$\text{pmol}\cdot\text{s}^{-1}\cdot 10^{-9} \text{ cells}$	$\text{zmol}\cdot\text{s}^{-1}\cdot\text{cell}^{-1}$	3
Cell number concentration, C_{Nce}	$10^6 \text{ cells}\cdot\text{mL}^{-1}$	$10^9 \text{ cells}\cdot\text{L}^{-1}$	
Mitochondrial protein concentration, C_{mte}	$0.1 \text{ mg}\cdot\text{mL}^{-1}$	$0.1 \text{ g}\cdot\text{L}^{-1}$	
Mass-specific flux, J_{m,O_2}	$\text{pmol}\cdot\text{s}^{-1}\cdot\text{mg}^{-1}$	$\text{nmol}\cdot\text{s}^{-1}\cdot\text{g}^{-1}$	4
Catabolic power, $P_{O_2,k}$	$\mu\text{W}\cdot 10^{-6} \text{ cells}$	$\text{pW}\cdot\text{cell}^{-1}$	1
Volume	1,000 L	m^3 (1,000 kg)	
	L	dm^3 (kg)	
	mL	cm^3 (g)	
	μL	mm^3 (mg)	
	fL	μm^3 (pg)	
Amount of substance concentration	$\text{M} = \text{mol}\cdot\text{L}^{-1}$	$\text{mol}\cdot\text{dm}^{-3}$	

1272

1273 1 pmol: picomole = 10^{-12} mol1274 2 amol: attomole = 10^{-18} mol1275 3 zmol: zeptomole = 10^{-21} mol1276 4 nmol: nanomole = 10^{-9} mol

1277

1278 ET-capacity in various human cell types including HEK 293, primary HUVEC and fibroblasts
 1279 ranges from 50 to $180 \text{ amol}\cdot\text{s}^{-1}\cdot\text{cell}^{-1}$, measured in intact cells in the noncoupled state (see
 1280 Gnaiger 2014). At $100 \text{ amol}\cdot\text{s}^{-1}\cdot\text{cell}^{-1}$ corrected for ROX (corresponding to a catabolic power
 1281 of $-48 \text{ pW}\cdot\text{cell}^{-1}$), the current across the mt-membranes, I_e , approximates $193 \text{ pA}\cdot\text{cell}^{-1}$ or 0.2

1282 nA per cell. See Rich (2003) for an extension of quantitative bioenergetics from the molecular
 1283 to the human scale, with a transmembrane proton flux equivalent to 520 A in an adult at a
 1284 catabolic power of -110 W. Modelling approaches illustrate the link between proton motive
 1285 force and currents (Willis *et al.* 2016). For NADH- and succinate-linked respiration, the
 1286 mechanistic P_»/O₂ ratio (referring to the full 4 electron reduction of O₂) is calculated at 20/3.7
 1287 and 12/3.7, respectively (Eq. 4) equal to 5.4 and 3.3. The classical P_»/O ratios (referring to the
 1288 2 electron reduction of 0.5 O₂) are 2.7 and 1.6 (Watt *et al.* 2010), in direct agreement with the
 1289 measured P_»/O ratio for succinate of 1.58 ± 0.02 (Gnaiger *et al.* 2000; for detailed reviews see
 1290 Wikström and Hummer 2012; Sazanov 2015),

$$1291 \quad P_{\gg}/O_2 = (H^+_{out}/O_2)/(H^+_{in}/P_{\gg}) \quad (\text{Eq. 4})$$

1292 In summary (**Fig. 1**),

$$1293 \quad J_{V,P_{\gg}} [\text{nmol}\cdot\text{s}^{-1}\cdot\text{L}^{-1}] = J_{V,O_2} \cdot (H^+_{out}/O_2)/(H^+_{in}/P_{\gg}) \quad (\text{Eq. 5.1})$$

$$1294 \quad J_{V,P_{\gg}} [\text{nmol}\cdot\text{s}^{-1}\cdot\text{L}^{-1}] = J_{V,O_2} \cdot (P_{\gg}/O_2) \quad (\text{Eq. 5.2})$$

1295 We consider isolated mitochondria as powerhouses and proton pumps as molecular machines
 1296 to relate experimental results to energy metabolism of the intact cell. The cellular P_»/O₂ based
 1297 on oxidation of glycogen is increased by the glycolytic (fermentative) substrate-level
 1298 phosphorylation of 3 P_»/Glyc, *i.e.*, 0.5 mol P_» for each mol O₂ consumed in the complete
 1299 oxidation of a mol glycosyl unit (Glyc). Adding 0.5 to the mitochondrial P_»/O₂ ratio of 5.4
 1300 yields a bioenergetic cell physiological P_»/O₂ ratio close to 6. Two NADH equivalents are
 1301 formed during glycolysis and transported from the cytosol into the mitochondrial matrix, either
 1302 by the malate-aspartate shuttle or by the glycerophosphate shuttle resulting in different
 1303 theoretical yield of ATP generated by mitochondria, the energetic cost of which potentially
 1304 must be taken into account. Considering also substrate-level phosphorylation in the TCA cycle,
 1305 this high P_»/O₂ ratio not only reflects proton translocation and OXPHOS studied in isolation,
 1306 but integrates mitochondrial physiology with energy transformation in the living cell (Gnaiger
 1307 1993a).

1308

1309 **5. Conclusions**

1310 MitoEAGLE can serve as a gateway to better diagnose mitochondrial respiratory defects
1311 linked to genetic variation, age-related health risks, sex-specific mitochondrial performance,
1312 lifestyle with its effects on degenerative diseases, and thermal and chemical environment. The
1313 present recommendations on coupling control states and rates, linked to the concept of the
1314 protonmotive force (Part 1) will be extended in a series of reports on pathway control of
1315 mitochondrial respiration, respiratory states in intact cells, and harmonization of experimental
1316 procedures.

1317

1318 Box 5: Mitochondrial and cell respiration

1319 Mitochondrial and cell respiration is the process of highly exergonic and exothermic energy
1320 transformation in which scalar redox reactions are coupled to vectorial ion translocation across
1321 a semipermeable membrane, which separates the small volume of a bacterial cell or
1322 mitochondrion from the larger volume of its surroundings. The electrochemical exergy can be
1323 partially conserved in the phosphorylation of ADP to ATP or in ion pumping, or dissipated in
1324 an electrochemical short-circuit. Respiration is thus clearly distinguished from fermentation as
1325 the counterpart of cellular core energy metabolism. Respiration is separated in mitochondrial
1326 preparations from the partial contribution of fermentative pathways of the intact cell. According
1327 to this definition, residual oxygen consumption, as measured after inhibition of mitochondrial
1328 electron transfer, does not belong to the class of catabolic reactions and is, therefore, subtracted
1329 from total oxygen consumption to obtain baseline-corrected respiration.

1330

1331 The optimal choice for expressing mitochondrial and cell respiration (**Box 5**) as O₂ flow
1332 per biological system, and normalization for specific tissue-markers (volume, mass, protein)
1333 and mitochondrial markers (volume, protein, content, mtDNA, activity of marker enzymes,

1334 respiratory reference state) is guided by the scientific question under study. Interpretation of
1335 the obtained data depends critically on appropriate normalization, and therefore reporting rates
1336 merely as $\text{nmol}\cdot\text{s}^{-1}$ is discouraged, since it restricts the analysis to intra-experimental
1337 comparison of relative (qualitative) differences. Expressing O_2 consumption per cell may not
1338 be possible when dealing with tissues. For studies with mitochondrial preparations, we
1339 recommend that normalizations be provided as far as possible: (1) on a per cell basis as O_2 flow
1340 (a biophysical normalization); (2) per g cell or tissue protein, or per cell or tissue mass as mass-
1341 specific O_2 flux (a cellular normalization); and (3) per mitochondrial marker as mt-specific flux
1342 (a mitochondrial normalization). With information on cell size and the use of multiple
1343 normalizations, maximum potential information is available (Renner *et al.* 2003; Wagner *et al.*
1344 2011; Gnaiger 2014). When using isolated mitochondria, mitochondrial protein is a frequently
1345 applied mitochondrial marker, the use of which is basically restricted to isolated mitochondria.
1346 Mitochondrial markers, such as citrate synthase activity as an enzymatic matrix marker, provide
1347 a link to the tissue of origin on the basis of calculating the mitochondrial yield, *i.e.*, the fraction
1348 of mitochondrial marker obtained from a unit mass of tissue.

1349

1350 **Acknowledgements**

1351 We thank M. Beno for management assistance. Supported by COST Action CA15203
1352 MitoEAGLE and K-Regio project MitoFit (EG).

1353 **Competing financial interests:** E.G. is founder and CEO of Oroboros Instruments, Innsbruck,
1354 Austria.

1355

1356 **6. References** (*incomplete; www links will be deleted in the final version*)

1357 Altmann R. Die Elementarorganismen und ihre Beziehungen zu den Zellen. Zweite vermehrte
1358 Auflage. Verlag Von Veit & Comp, Leipzig 1894;160 pp. -

1359 www.mitoeagle.org/index.php/Altmann_1894_Verlag_Von_Veit_%26_Comp

- 1360 Birkedal R, Laasmaa M, Vendelin M. The location of energetic compartments affects
1361 energetic communication in cardiomyocytes. *Front Physiol* 2014;5:376. doi:
1362 10.3389/fphys.2014.00376. eCollection 2014. PMID: 25324784
- 1363 Breton S, Beaupré HD, Stewart DT, Hoeh WR, Blier PU. The unusual system of doubly
1364 uniparental inheritance of mtDNA: isn't one enough? *Trends Genet* 2007;23:465-74.
- 1365 Brown GC. Control of respiration and ATP synthesis in mammalian mitochondria and cells.
1366 *Biochem J* 1992;284:1-13. - www.mitoeagle.org/index.php/Brown_1992_Biochem_J
- 1367 Campos JC, Queliconi BB, Bozi LHM, Bechara LRG, Dourado PMM, Andres AM, Jannig
1368 PR, Gomes KMS, Zambelli VO, Rocha-Resende C, Guatimosim S, Brum PC, Mochly-
1369 Rosen D, Gottlieb RA, Kowaltowski AJ, Ferreira JCB. Exercise reestablishes
1370 autophagic flux and mitochondrial quality control in heart failure. *Autophagy*
1371 2017;13:1304-317.
- 1372 Chance B, Williams GR. Respiratory enzymes in oxidative phosphorylation. I. Kinetics of
1373 oxygen utilization. *J Biol Chem* 1955a;217:383-93. -
1374 http://www.mitoeagle.org/index.php/Chance_1955_J_Biol_Chem-I
- 1375 Chance B, Williams GR. Respiratory enzymes in oxidative phosphorylation: III. The steady
1376 state. *J Biol Chem* 1955b;217:409-27. -
1377 www.mitoeagle.org/index.php/Chance_1955_J_Biol_Chem-III
- 1378 Chance B, Williams GR. Respiratory enzymes in oxidative phosphorylation. IV. The
1379 respiratory chain. *J Biol Chem* 1955c;217:429-38. -
1380 www.mitoeagle.org/index.php/Chance_1955_J_Biol_Chem-IV
- 1381 Chance B, Williams GR. The respiratory chain and oxidative phosphorylation. *Adv Enzymol*
1382 *Relat Subj Biochem* 1956;17:65-134. -
1383 www.mitoeagle.org/index.php/Chance_1956_Adv_Enzymol_Relat_Subj_Biochem
- 1384 Cobb LJ, Lee C, Xiao J, Yen K, Wong RG, Nakamura HK, Mehta HH, Gao Q, Ashur C,
1385 Huffman DM, Wan J, Muzumdar R, Barzilai N, Cohen P. Naturally occurring

- 1386 mitochondrial-derived peptides are age-dependent regulators of apoptosis, insulin
1387 sensitivity, and inflammatory markers. *Aging* (Albany NY) 2016;8:796-809.
- 1388 Cohen ER, Cvitas T, Frey JG, Holmström B, Kuchitsu K, Marquardt R, Mills I, Pavese F,
1389 Quack M, Stohner J, Strauss HL, Takami M, Thor HL. Quantities, units and symbols in
1390 physical chemistry, IUPAC Green Book 2008;3rd Edition, 2nd Printing, IUPAC & RSC
1391 Publishing, Cambridge. -
1392 www.mitoeagle.org/index.php/Cohen_2008_IUPAC_Green_Book
- 1393 Cooper H, Hedges LV, Valentine JC (eds). The handbook of research synthesis and meta-
1394 analysis. Russell Sage Foundation 2009.
- 1395 Coopersmith J. Energy, the subtle concept. The discovery of Feynman's blocks from Leibnitz
1396 to Einstein. Oxford University Press 2010;400 pp.
- 1397 Cummins J. Mitochondrial DNA in mammalian reproduction. *Rev Reprod* 1998;3:172–82.
- 1398 Dai Q, Shah AA, Garde RV, Yonish BA, Zhang L, Medvitz NA, Miller SE, Hansen EL, Dunn
1399 CN, Price TM. A truncated progesterone receptor (PR-M) localizes to the
1400 mitochondrion and controls cellular respiration. *Mol Endocrinol* 2013;27:741-53.
- 1401 Duarte FV, Palmeira CM, Rolo AP. The role of microRNAs in mitochondria: small players
1402 acting wide. *Genes* (Basel) 2014;5:865-86.
- 1403 Dufour S, Rousse N, Canioni P, Diolez P. Top-down control analysis of temperature effect on
1404 oxidative phosphorylation. *Biochem J* 1996;314:743-51.
- 1405 Ernster L, Schatz G Mitochondria: a historical review. *J Cell Biol* 1981;91:227s-55s. -
1406 www.mitoeagle.org/index.php/Ernster_1981_J_Cell_Biol
- 1407 Estabrook RW. Mitochondrial respiratory control and the polarographic measurement of
1408 ADP:O ratios. *Methods Enzymol* 1967;10:41-7. -
1409 www.mitoeagle.org/index.php/Estabrook_1967_Methods_Enzymol
- 1410 Faber C, Zhu ZJ, Castellino S, Wagner DS, Brown RH, Peterson RA, Gates L, Barton J,
1411 Bickett M, Hagerty L, Kimbrough C, Sola M, Bailey D, Jordan H, Elangbam CS.

- 1412 Cardiolipin profiles as a potential biomarker of mitochondrial health in diet-induced
1413 obese mice subjected to exercise, diet-restriction and ephedrine treatment. *J Appl*
1414 *Toxicol* 2014;34:1122-9.
- 1415 Fell D. *Understanding the control of metabolism*. Portland Press 1997.
- 1416 Garlid KD, Semrad C, Zinchenko V. Does redox slip contribute significantly to mitochondrial
1417 respiration? In: Schuster S, Rigoulet M, Ouhabi R, Mazat J-P (eds) *Modern trends in*
1418 *biothermokinetics*. Plenum Press, New York, London 1993;287-93.
- 1419 Gerö D, Szabo C. Glucocorticoids suppress mitochondrial oxidant production via
1420 upregulation of uncoupling protein 2 in hyperglycemic endothelial cells. *PLoS One*
1421 2016;11:e0154813.
- 1422 Gnaiger E. Efficiency and power strategies under hypoxia. Is low efficiency at high glycolytic
1423 ATP production a paradox? In: *Surviving Hypoxia: Mechanisms of Control and*
1424 *Adaptation*. Hochachka PW, Lutz PL, Sick T, Rosenthal M, Van den Thillart G (eds.)
1425 CRC Press, Boca Raton, Ann Arbor, London, Tokyo 1993a:77-109. -
1426 www.mitoeagle.org/index.php/Gnaiger_1993_Hypoxia
- 1427 Gnaiger E. Nonequilibrium thermodynamics of energy transformations. *Pure Appl Chem*
1428 1993b;65:1983-2002. - www.mitoeagle.org/index.php/Gnaiger_1993_Pure_Appl_Chem
- 1429 Gnaiger E. Bioenergetics at low oxygen: dependence of respiration and phosphorylation on
1430 oxygen and adenosine diphosphate supply. *Respir Physiol* 2001;128:277-97. -
1431 www.mitoeagle.org/index.php/Gnaiger_2001_Respir_Physiol
- 1432 Gnaiger E. *Mitochondrial pathways and respiratory control. An introduction to OXPHOS*
1433 *analysis*. 4th ed. *Mitochondr Physiol Network* 2014;19.12. Oroboros MiPNet
1434 Publications, Innsbruck:80 pp. -
1435 www.mitoeagle.org/index.php/Gnaiger_2014_MitoPathways

- 1436 Gnaiger E. Capacity of oxidative phosphorylation in human skeletal muscle. New
1437 perspectives of mitochondrial physiology. *Int J Biochem Cell Biol* 2009;41:1837-45. -
1438 www.mitoeagle.org/index.php/Gnaiger_2009_Int_J_Biochem_Cell_Biol
- 1439 Gnaiger E, Méndez G, Hand SC. High phosphorylation efficiency and depression of
1440 uncoupled respiration in mitochondria under hypoxia. *Proc Natl Acad Sci USA*
1441 2000;97:11080-5. -
1442 www.mitoeagle.org/index.php/Gnaiger_2000_Proc_Natl_Acad_Sci_U_S_A
- 1443 Greggio C, Jha P, Kulkarni SS, Lagarrigue S, Broskey NT, Boutant M, Wang X, Conde
1444 Alonso S, Ofori E, Auwerx J, Cantó C, Amati F. Enhanced respiratory chain
1445 supercomplex formation in response to exercise in human skeletal muscle. *Cell Metab*
1446 2017;25:301-11. - http://www.mitoeagle.org/index.php/Greggio_2017_Cell_Metab
- 1447 Hofstadter DR. Gödel, Escher, Bach: An eternal golden braid. A metaphorical fugue on minds
1448 and machines in the spirit of Lewis Carroll. Harvester Press 1979;499 pp. -
1449 www.mitoeagle.org/index.php/Hofstadter_1979_Harvester_Press
- 1450 Illaste A, Laasmaa M, Peterson P, Vendelin M. Analysis of molecular movement reveals
1451 latticelike obstructions to diffusion in heart muscle cells. *Biophys J* 2012;102:739-48. -
1452 PMID: 22385844
- 1453 Jasienski M, Bazzaz FA. The fallacy of ratios and the testability of models in biology. *Oikos*
1454 1999;84:321-26.
- 1455 Jepihhina N, Beraud N, Sepp M, Birkedal R, Vendelin M. Permeabilized rat cardiomyocyte
1456 response demonstrates intracellular origin of diffusion obstacles. *Biophys J*
1457 2011;101:2112-21. - PMID: 22067148
- 1458 Klepinin A, Ounpuu L, Guzun R, Chekulayev V, Timohhina N, Tepp K, Shevchuk I,
1459 Schlattner U, Kaambre T. Simple oxygraphic analysis for the presence of adenylate
1460 kinase 1 and 2 in normal and tumor cells. *J Bioenerg Biomembr* 2016;48:531-48. -
1461 http://www.mitoeagle.org/index.php/Klepinin_2016_J_Bioenerg_Biomembr

- 1462 Klingenberg M. UCP1 - A sophisticated energy valve. *Biochimie* 2017;134:19-27
- 1463 Koit A, Shevchuk I, Ounpuu L, Klepinin A, Chekulayev V, Timohhina N, Tepp K, Puurand
1464 M, Truu L, Heck K, Valvere V, Guzun R, Kaambre T. Mitochondrial respiration in
1465 human colorectal and breast cancer clinical material is regulated differently. *Oxid Med*
1466 *Cell Longev* 2017;1372640. -
1467 http://www.mitoeagle.org/index.php/Koit_2017_Oxid_Med_Cell_Longev
- 1468 Komlódi T, Tretter L. Methylene blue stimulates substrate-level phosphorylation catalysed by
1469 succinyl-CoA ligase in the citric acid cycle. *Neuropharmacology* 2017;123:287-98. -
1470 www.mitoeagle.org/index.php/Komlodi_2017_Neuropharmacology
- 1471 Lane N. Power, sex, suicide: Mitochondria and the meaning of life. Oxford University Press
1472 2005;354 pp.
- 1473 Larsen S, Nielsen J, Neigaard Nielsen C, Nielsen LB, Wibrand F, Stride N, Schroder HD,
1474 Boushel RC, Helge JW, Dela F, Hey-Mogensen M. Biomarkers of mitochondrial
1475 content in skeletal muscle of healthy young human subjects. *J Physiol* 590;2012:3349-
1476 60. - http://www.mitoeagle.org/index.php/Larsen_2012_J_Physiol
- 1477 Lee C, Zeng J, Drew BG, Sallam T, Martin-Montalvo A, Wan J, Kim SJ, Mehta H, Hevener
1478 AL, de Cabo R, Cohen P. The mitochondrial-derived peptide MOTS-c promotes
1479 metabolic homeostasis and reduces obesity and insulin resistance. *Cell Metab*
1480 2015;21:443-54.
- 1481 Lee SR, Kim HK, Song IS, Youm J, Dizon LA, Jeong SH, Ko TH, Heo HJ, Ko KS, Rhee BD,
1482 Kim N, Han J. Glucocorticoids and their receptors: insights into specific roles in
1483 mitochondria. *Prog Biophys Mol Biol* 2013;112:44-54.
- 1484 Leek BT, Mudaliar SR, Henry R, Mathieu-Costello O, Richardson RS. Effect of acute
1485 exercise on citrate synthase activity in untrained and trained human skeletal muscle. *Am*
1486 *J Physiol Regul Integr Comp Physiol* 2001;280:R441-7.

- 1487 Lemieux H, Blier PU, Gnaiger E. Remodeling pathway control of mitochondrial respiratory
1488 capacity by temperature in mouse heart: electron flow through the Q-junction in
1489 permeabilized fibers. *Sci Rep* 2017;7:2840. -
1490 www.mitoeagle.org/index.php/Lemieux_2017_Sci_Rep
- 1491 Lenaz G, Tioli G, Falasca AI, Genova ML. Respiratory supercomplexes in mitochondria. In:
1492 Mechanisms of primary energy trasduction in biology. M Wikstrom (ed) Royal Society
1493 of Chemistry Publishing, London, UK 2017:296-337 (in press)
- 1494 Margulis L. Origin of eukaryotic cells. New Haven: Yale University Press 1970.
- 1495 Meinild Lundby AK, Jacobs RA, Gehrig S, de Leur J, Hauser M, Bonne TC, Flück D,
1496 Dandanell S, Kirk N, Kaech A, Ziegler U, Larsen S, Lundby C. Exercise training
1497 increases skeletal muscle mitochondrial volume density by enlargement of existing
1498 mitochondria and not de novo biogenesis. *Acta Physiol (Oxf)* 2017;[Epub ahead of
1499 print].
- 1500 Menshikova EV, Ritov VB, Fairfull L, Ferrell RE, Kelley DE, Goodpaster BH. Effects of
1501 exercise on mitochondrial content and function in aging human skeletal muscle. *J*
1502 *Gerontol A Biol Sci Med Sci* 2006;61:534-40.
- 1503 Menshikova EV, Ritov VB, Ferrell RE, Azuma K, Goodpaster BH, Kelley DE.
1504 Characteristics of skeletal muscle mitochondrial biogenesis induced by moderate-
1505 intensity exercise and weight loss in obesity. *J Appl Physiol (1985)* 2007;103:21-7.
- 1506 Menshikova EV, Ritov VB, Toledo FG, Ferrell RE, Goodpaster BH, Kelley DE. Effects of
1507 weight loss and physical activity on skeletal muscle mitochondrial function in obesity.
1508 *Am J Physiol Endocrinol Metab* 2005;288:E818-25.
- 1509 Miller GA. The science of words. Scientific American Library New York 1991;276 pp. -
1510 www.mitoeagle.org/index.php/Miller_1991_Scientific_American_Library

- 1511 Mitchell P. Chemiosmotic coupling in oxidative and photosynthetic phosphorylation *Biochim*
1512 *Biophys Acta Bioenergetics* 2011;1807:1507-38. -
1513 <http://www.sciencedirect.com/science/article/pii/S0005272811002283>
- 1514 Mitchell P, Moyle J. Respiration-driven proton translocation in rat liver mitochondria.
1515 *Biochem J* 1967;105:1147-62. -
1516 www.mitoeagle.org/index.php/Mitchell_1967_Biochem_J
- 1517 Mogensen M, Sahlin K, Fernström M, Glinborg D, Vind BF, Beck-Nielsen H, Højlund K.
1518 Mitochondrial respiration is decreased in skeletal muscle of patients with type 2
1519 diabetes. *Diabetes* 2007;56:1592-9.
- 1520 Moreno M, Giacco A, Di Munno C, Goglia F. Direct and rapid effects of 3,5-diiodo-L-
1521 thyronine (T2). *Mol Cell Endocrinol* 2017;7207:30092-8.
- 1522 Morrow RM, Picard M, Derbeneva O, Leipzig J, McManus MJ, Gouspillou G, Barbat-Artigas
1523 S, Dos Santos C, Hepple RT, Murdock DG, Wallace DC. Mitochondrial energy
1524 deficiency leads to hyperproliferation of skeletal muscle mitochondria and enhanced
1525 insulin sensitivity. *Proc Natl Acad Sci U S A* 2017;114:2705-10. -
1526 www.mitoeagle.org/index.php/Morrow_2017_Proc_Natl_Acad_Sci_U_S_A
- 1527 Nicholls DG, Ferguson S. *Bioenergetics 4*. Elsevier 2013.
- 1528 Paradies G, Paradies V, De Benedictis V, Ruggiero FM, Petrosillo G. Functional role of
1529 cardiolipin in mitochondrial bioenergetics. *Biochim Biophys Acta* 2014;1837:408-17. -
1530 http://www.mitoeagle.org/index.php/Paradies_2014_Biochim_Biophys_Acta
- 1531 Pesta D, Hoppel F, Macek C, Messner H, Faulhaber M, Kobel C, Parson W, Bartscher M,
1532 Schocke M, Gnaiger E. Similar qualitative and quantitative changes of mitochondrial
1533 respiration following strength and endurance training in normoxia and hypoxia in
1534 sedentary humans. *Am J Physiol Regul Integr Comp Physiol* 2011;301:R1078-87.
- 1535 Price TM, Dai Q. The Role of a Mitochondrial Progesterone Receptor (PR-M) in
1536 Progesterone Action. *Semin Reprod Med.* 2015;33:185-94.

- 1537 Prigogine I. Introduction to thermodynamics of irreversible processes. Interscience, New
1538 York, 1967;3rd ed.
- 1539 Puchowicz MA, Varnes ME, Cohen BH, Friedman NR, Kerr DS, Hoppel CL. Oxidative
1540 phosphorylation analysis: assessing the integrated functional activity of human skeletal
1541 muscle mitochondria – case studies. *Mitochondrion* 2004;4:377-85. -
1542 www.mitoeagle.org/index.php/Puchowicz_2004_Mitochondrion
- 1543 Puntschart A, Claassen H, Jostarndt K, Hoppeler H, Billeter R. mRNAs of enzymes involved
1544 in energy metabolism and mtDNA are increased in endurance-trained athletes. *Am J*
1545 *Physiol* 1995;269:C619-25.
- 1546 Quiros PM, Mottis A, Auwerx J. Mitonuclear communication in homeostasis and stress. *Nat*
1547 *Rev Mol Cell Biol* 2016;17:213-26.
- 1548 Reichmann H, Hoppeler H, Mathieu-Costello O, von Bergen F, Pette D. Biochemical and
1549 ultrastructural changes of skeletal muscle mitochondria after chronic electrical
1550 stimulation in rabbits. *Pflugers Arch* 1985;404:1-9.
- 1551 Renner K, Amberger A, Konwalinka G, Gnaiger E. Changes of mitochondrial respiration,
1552 mitochondrial content and cell size after induction of apoptosis in leukemia cells.
1553 *Biochim Biophys Acta* 2003;1642:115-23. -
1554 www.mitoeagle.org/index.php/Renner_2003_Biochim_Biophys_Acta
- 1555 Rich P. Chemiosmotic coupling: The cost of living. *Nature* 2003;421:583. -
1556 www.mitoeagle.org/index.php/Rich_2003_Nature
- 1557 Rostovtseva TK, Sheldon KL, Hassanzadeh E, Monge C, Saks V, Bezrukov SM, Sackett DL.
1558 Tubulin binding blocks mitochondrial voltage-dependent anion channel and regulates
1559 respiration. *Proc Natl Acad Sci USA* 2008;105:18746-51. -
1560 www.mitoeagle.org/index.php/Rostovtseva_2008_Proc_Natl_Acad_Sci_U_S_A

- 1561 Rustin P, Parfait B, Chretien D, Bourgeron T, Djouadi F, Bastin J, Rötig A, Munnich A.
1562 Fluxes of nicotinamide adenine dinucleotides through mitochondrial membranes in
1563 human cultured cells. *J Biol Chem* 1996;271:14785-90.
- 1564 Saks VA, Veksler VI, Kuznetsov AV, Kay L, Sikk P, Tiivel T, Tranqui L, Olivares J, Winkler
1565 K, Wiedemann F, Kunz WS. Permeabilised cell and skinned fiber techniques in studies
1566 of mitochondrial function in vivo. *Mol Cell Biochem* 1998;184:81-100. -
1567 http://www.mitoeagle.org/index.php/Saks_1998_Mol_Cell_Biochem
- 1568 Salabei JK, Gibb AA, Hill BG. Comprehensive measurement of respiratory activity in
1569 permeabilized cells using extracellular flux analysis. *Nat Protoc* 2014;9:421-38.
- 1570 Sazanov LA. A giant molecular proton pump: structure and mechanism of respiratory
1571 complex I. *Nat Rev Mol Cell Biol* 2015;16:375-88. -
1572 www.mitoeagle.org/index.php/Sazanov_2015_Nat_Rev_Mol_Cell_Biol
- 1573 Schneider TD. Claude Shannon: biologist. The founder of information theory used biology to
1574 formulate the channel capacity. *IEEE Eng Med Biol Mag* 2006;25:30-3.
- 1575 Schönfeld P, Dymkowska D, Wojtczak L. Acyl-CoA-induced generation of reactive oxygen
1576 species in mitochondrial preparations is due to the presence of peroxisomes. *Free Radic*
1577 *Biol Med* 2009;47:503-9.
- 1578 Schrödinger E. *What is life? The physical aspect of the living cell.* Cambridge Univ Press,
1579 1944. - www.mitoeagle.org/index.php/Gnaiger_1994_BTK
- 1580 Schultz J, Wiesner RJ. Proliferation of mitochondria in chronically stimulated rabbit skeletal
1581 muscle--transcription of mitochondrial genes and copy number of mitochondrial DNA.
1582 *J Bioenerg Biomembr* 2000;32:627-34.
- 1583 Simson P, Jepihhina N, Laasmaa M, Peterson P, Birkedal R, Vendelin M. Restricted ADP
1584 movement in cardiomyocytes: Cytosolic diffusion obstacles are complemented with a
1585 small number of open mitochondrial voltage-dependent anion channels. *J Mol Cell*
1586 *Cardiol* 2016;97:197-203. - PMID: 27261153

- 1587 Stucki JW, Ineichen EA. Energy dissipation by calcium recycling and the efficiency of
1588 calcium transport in rat-liver mitochondria. *Eur J Biochem* 1974;48:365-75.
- 1589 Tonkonogi M, Harris B, Sahlin K. Increased activity of citrate synthase in human skeletal
1590 muscle after a single bout of prolonged exercise. *Acta Physiol Scand* 1997;161:435-6.
- 1591 Waczulikova I, Habodaszova D, Cagalinec M, Ferko M, Ulicna O, Mateasik A, Sikurova L,
1592 Ziegelhöffer A. Mitochondrial membrane fluidity, potential, and calcium transients in
1593 the myocardium from acute diabetic rats. *Can J Physiol Pharmacol* 2007;85:372-81.
- 1594 Wagner BA, Venkataraman S, Buettner GR. The rate of oxygen utilization by cells. *Free*
1595 *Radic Biol Med.* 2011;51:700-712.
1596 <http://dx.doi.org/10.1016/j.freeradbiomed.2011.05.024> PMID: PMC3147247
- 1597 Wang H, Hiatt WR, Barstow TJ, Brass EP. Relationships between muscle mitochondrial
1598 DNA content, mitochondrial enzyme activity and oxidative capacity in man: alterations
1599 with disease. *Eur J Appl Physiol Occup Physiol* 1999;80:22-7.
- 1600 Watt IN, Montgomery MG, Runswick MJ, Leslie AG, Walker JE. Bioenergetic cost of
1601 making an adenosine triphosphate molecule in animal mitochondria. *Proc Natl Acad Sci*
1602 *U S A* 2010;107:16823-7. -
1603 www.mitoeagle.org/index.php/Watt_2010_Proc_Natl_Acad_Sci_U_S_A
- 1604 Weibel ER, Hoppeler H. Exercise-induced maximal metabolic rate scales with muscle aerobic
1605 capacity. *J Exp Biol* 2005;208:1635-44.
- 1606 White DJ, Wolff JN, Pierson M, Gemmell NJ. Revealing the hidden complexities of mtDNA
1607 inheritance. *Mol Ecol* 17; 2008:4925-42.
- 1608 Wikström M, Hummer G. Stoichiometry of proton translocation by respiratory complex I and
1609 its mechanistic implications. *Proc Natl Acad Sci U S A* 2012;109:4431-6. -
1610 www.mitoeagle.org/index.php/Wikstroem_2012_Proc_Natl_Acad_Sci_U_S_A
- 1611 Willis WT, Jackman MR, Messer JJ, Kuzmiak-Glancy S, Glancy B. A simple hydraulic
1612 analog model of oxidative phosphorylation. *Med Sci Sports Exerc.* 2016;48:990-1000.